



TALLINN UNIVERSITY OF TECHNOLOGY

SCHOOL OF ENGINEERING

Department of Electrical Power Engineering and Mechatronics

# **DESIGN OF A TOPOLOGY OPTIMIZED HEATSINK FOR A DRONE MOTOR**

## **TOPOLOOGIA OPTIMEERITUD JAHUTI LOOMINE DROONI MOOTORILE**

MASTER THESIS

Student: Sten Erik Aunpu

Student code: MAHM204814

Supervisor: Martin Sarap, Early Stage Researcher

Tallinn, 2023

## **AUTHOR'S DECLARATION**

Hereby I declare, that I have written this thesis independently.

No academic degree has been applied for based on this material. All works, major viewpoints and data of the other authors used in this thesis have been referenced.

"18" May 2023.

Author: Sten Erik Aunpu

/signature /

Thesis is in accordance with terms and requirements.

"18" May 2023.

Supervisor: Martin Sarap

/signature/

Accepted for defence

"....." .....202... .

Chairman of theses defence commission: .....

/name and signature/

## **Non-exclusive Licence for Publication and Reproduction of Graduation Thesis<sup>1</sup>**

I, Sten Erik Aunpu (*date of birth: 13/08/1998*) hereby

1. grant Tallinn University of Technology (TalTech) a non-exclusive license for my thesis  
" Design of a topology optimized heatsink for a drone motor"

supervised by

Martin Sarap – Early Stage Researcher, Tallinn University of Technology,

- 1.1 reproduced for the purposes of preservation and electronic publication, incl. to be entered in the digital collection of TalTech library until expiry of the term of copyright;

- 1.2 published via the web of TalTech, incl. to be entered in the digital collection of TalTech library until expiry of the term of copyright.

- 1.3 I am aware that the author also retains the rights specified in clause 1 of this license.

2. I confirm that granting the non-exclusive license does not infringe third persons' intellectual property rights, the rights arising from the Personal Data Protection Act or rights arising from other legislation.

\_\_\_\_\_ (*signature*)

18. May 2023 (*date*)

---

<sup>1</sup> *The non-exclusive licence is not valid during the validity of access restriction indicated in the student's application for restriction on access to the graduation thesis that has been signed by the school's dean, except in case of the university's right to reproduce the thesis for preservation purposes only. If a graduation thesis is based on the joint creative activity of two or more persons and the co-author(s) has/have not granted, by the set deadline, the student defending his/her graduation thesis consent to reproduce and publish the graduation thesis in compliance with clauses 1.1 and 1.2 of the non-exclusive licence, the non-exclusive license shall not be valid for the period.*

## ABSTRACT

*Author:* Sten Erik Aunpu

*Type of the work:* Master Thesis

*Title:* Design of a topology optimized heatsink for a drone motor

*Date:* 18.05.2023

68 pages (the number of thesis pages including appendices)

*University:* Tallinn University of Technology

*School:* School of Engineering

*Department:* Department of Electrical Power Engineering and Mechatronics

*Supervisor(s) of the thesis:* Early Stage Researcher Martin Sarap

*Consultant(s):*

*Abstract:*

This thesis aims to create and validate topology optimized heatsinks designs for motors of small drones. The work is done out both Taltech's faculties interest in electrical motor cooling solutions and authors interest in how additive manufacturing can be used for improving mechatronics solutions.

The works is divided in to three main chapters. First chapters researches the background of topology optimization and how it could be applied to optimization of heatsinks. Information gathered in the first chapter is used as the basis for the optimization process described and used in the second chapter. The second chapter also covers the testing of gotten heatsinks designs in a simulated environment. The final chapters focuses on the testing the mentioned heatsink designs in real-world and analysing if and what benefits TO offers.

As a result of this thesis variety of drone motor heatsink designs were created, manufactured, and tested. Topology optimization was used to create the designs. Test were conducted in both simulated and real environments. The heatsinks were manufactured by 3D printing metal. Test results showed that the created TO heatsinks are more effective than parametrically optimized heatsinks while also showing potential benefits to the motors performance. The most optimal heatsink design was selected out of based on the testing results.

*Keywords:* drone, heatsink, cooling, topology optimization, SIMP, additive manufacturing, SLM, COMSOL, physics simulation.

# LÕPUTÖÖ LÜHIKOKKUVÕTE

*Autor:* Sten Erik Aunpu

*Lõputöö liik:* Magistritöö

*Töö pealkiri:* Topoloogia optimeeritud jahuti loomine drooni mootorile

*Kuupäev:*

68 lk (*lõputöö lehekülgede arv koos lisadega*)

18.05.2023

*Ülikool:* Tallinna Tehnikaülikool

*Teaduskond:* Inseneriteaduskond

*Instituut:* Elektroenergeetika ja mehhatroonika instituut

*Töö juhendaja(d):* Doktorant-Nooremteadur Martin Sarap

*Töö konsultant (konsultandid):*

*Sisu kirjeldus:*

Antud lõputöö eesmärgiks oli luua topoloogia optimeerimisega jahutite disainid väikestele drooni mootoritele ja need siis valideerida. Töö teema valimisel lähtuti nii Taltech'i töötajate huvist elektrimootorite jahutuslahenduste vastu kui ka autori enda huvist, kuidas on võimalik kasutada 3D-printimist mehhatroonika lahenduste täiustamisel.

Töö on jagatud kolme põhipeatükki. Esimeses peatükis uuritakse topoloogia optimeerimise tausta ja selle rakendatavust jahutusradiaatorite optimeerimisel. Esimeses peatükis kogutud teavet kasutatakse teises peatükis kirjeldatud optimeerimisprotsessi loomise ja konfigureerimise aluseks. Teises peatükis käsitletakse ka loodud jahutite disainide testimist simuleeritud keskkonnas. Viimane peatükk keskendub eelnevalt mainitud jahututite testimisele reaalses keskkonnas ning TO eeliste ja kasutatavuse analüüsile.

Selle magistritöö tulemusena loodi, toodeti ja testiti erinevaid drooni mootorite radiaatoreid. Disainide loomisel kasutati topoloogia optimeerimist. Testid viidi läbi nii simuleeritud kui reaalses keskkonnas. Radiaatorid valmistati metalli 3D-printimisega. Katsetulemused näitasid, et loodud TO radiaatorid on tõhusamad kui parameetriliselt optimeeritud variandid, näidates samal ajal ka potentsiaalset kasu mootori jõudlusele. Tulemuste põhjal valiti välja loodud disainidest kõige optimaalsem

*Märksõnad:* droon, radiaator, jahutus, topoloogiline optimeerimine, SIMP, 3D printimine, SLM, COMSOL, füüsika simulatsioon.

# THESIS TASK

Thesis title in English: **Design of a Topology Optimized Heatsink for a Drone Motor**  
**Topoloogiaoptimeeritud jahuti loomine drooni mootorile**

Thesis title in Estonian: **mootorile**

Student: **Sten Erik Aunpu, 204814MAHM**

Programme: **Mechatronics, MAHM**

Type of the work: **Master's Thesis**

Supervisor of the thesis: **Martin Sarap, Early Stage Researcher – Department of Electrical Power Engineering and Mechatronics**

Co-supervisor of the thesis:  
(company, position and contact)

Validity period of the thesis task: 2022/2023 2022/2023 Spring

Submission deadline of the thesis: **18.05.2023**

---

Supervisor (signature)

---

Student (signature)

---

Head of programme (signature)

---

Co-supervisor (signature)

## 1. Reasons for choosing the topic

The thesis topic choice was motivated by the universities desire to see if and how they can improve the performance of their small drones in different projects. The chosen topic also allows the use and research into technologies and applications related to additive manufacturing that the author is personally interested in.

Drones have become popular as both hobbyist and professional devices in different fields. To support their adoption to different applications, standardized frameworks [1] have been developed. As these aerial devices/systems have evolved, they have also gotten much smaller while having increased computational and/or electrical power. Smaller drones are especially prevalent in household use or more complex swarm-based solutions. Swarm-based solutions have, for example, been proposed for such military

application as missile countering [2]. A large amount power in a small area means that increased attention must be paid to the thermal management of these system.

The small and commonly used drone motors, for example CL1020 and CL8520, used in university projects do not include heatsinks. The only heat dissipation element these coreless DC motors have is the outer metal enclosure of the motor. Due to a lack of cooling the performance of the motors is thermally limited.

As heatsinks for drones need to be lightweight and effective, topology optimization and additive manufacturing can be ideal technologies to achieve the desired design results. 3D printing allows the realization of the complex organic designs created by topology optimization. While research on using these technologies together has been mostly centred on optimizing mechanical structures, like in [3], there has been a shift towards other applications like heatsink design [4][5] only in recent years.

## **2. Thesis objective**

The aim of this thesis is to design an optimized heatsink for a small drone motor to increase its performance. Topology optimization will be used in the design process. The optimized heatsink design will be manufactured with SLM (Selective laser Melting) and then validated with testing.

## **3. List of sub-questions:**

The thesis aims to answer the following sub-questions:

- If and how much does the heatsink increase the drone motor performance?
- Do the simulation results match with the real-world testing?
- Does the optimized heatsink provide other benefits?
- Do the benefits of the designed heatsink justify themselves for actual use?

## **4. Basic data:**

To solve the stated objectives the following data will be needed:

- Research on similar existing design and optimization solutions.
- Properties of the drone motor.
- Computer generated heatsink designs.
- Simulated heatsink performance results.
- Results from laboratory testing.

Data will be gathered from:

- Previous research.
- Datasheets.
- Software examples or manuals.
- Computer simulations.
- Laboratory testing.

## **5. Research methods**

The optimization process will be carried out using the COMSOL Multiphysics simulation software. This program allows the modelling of different physics simulations, including thermal transfer simulations that will be needed to reach the desired result for this thesis.

First, a model will be created that represents the drone motor including its heat losses, air current created by the propeller etc. This will be used as the basis for the design process.

Then, optimization methods will be applied to a design space around the motor stator. The resulting design will then be validated using the simulation of a drone motor. Multiple optimized designs will be created by tweaking the optimization process. The design(s) with best results will be manufactured using SLM 3D printing and tested in the university laboratory.

Laboratory tests will be used to measure the heat dissipation capability of different heatsink designs. This will validate if the designs gotten using optimization have similar thermal performance in real-world as they had in the simulated environment. Furthermore, the effects of the heatsink on motors potential lift generation will be measured to see how large the performance benefits are.

## **6. Graphical material**

The main work will contain the following graphical elements:

- Visual representations of simulations results.
- Tables for summarizing simulation and testing results.
- Pictures of the testing setup.
- Pictures taken during testing.

Additional graphical material that is not directly required for achieving the aims of the thesis will be included in the appendixes.

## 7. Thesis structure

Structure of the thesis will be in the following chapters:

- Introduction
- Literature review
  - Review of exiting research on the topic.
  - Research on drones and their motors.
  - Research into designing of heatsinks.
  - Design consideration for heatsinks in drone application.
  - Existing heatsink design optimization methods.
  - Feasibility of additive manufacturing for heatsink production.
  - Conclusion of literature review.
- Optimization of heatsink design
  - Simulation setup description.
  - Description of the optimization process and methodology.
  - Results gotten from optimization and simulations.
  - Summary of how the designs will be turned into real-world objects.
- Testing of the optimized heatsink
  - Description of the testing setup and methodology
  - Conclusion from the results.
  - Suggestions for further developments
- Conclusion

## 8. References

The main sources for this thesis will be research articles covering the design and optimization of active cooling/heatsink solutions. Also, sources covering topology optimization, drones and additive manufacturing will be used.

- [1] "IEEE Standard for Drone Applications Framework," in IEEE Std 1936.1-2021
- [2] L. Szarka and I. Harmati, "Swarm based drone umbrellas to counter missiles," 2020 23rd International Symposium on Measurement and Control in Robotics (ISMCR), 2020
- [3] Zifan Fang, Lei Yang, Daojia Du, Kongde He, Dalin Zhu and Yi Zhang, "Study on multi-objective topology optimization design for support structure," 2010 International Conference on Mechanic Automation and Control Engineering, 2010
- [4] F. Lange, C. Hein, G. Li, C. Emmelmann, " Numerical optimization of active heat sinks considering restrictions of selective laser melting", 2018 Fraunhofer Research Institution for Additive Manufacturing Technologies IAPT, Hamburg, Germany

[5] M. S. Santhanakrishnan, T. Tilford and C. Bailey, "Multi-Material Heatsink Design Using Level-Set Topology Optimization," in IEEE Transactions on Components, Packaging and Manufacturing Technology, vol. 9, no. 8, pp. 1504-1513, Aug. 2019

## 9. Thesis consultants

If needed experts of topics related to this thesis will be consulted.

## 10. Work stages and schedule

Following table contains thesis work stages with their respective schedule:

<b>Work stage/Activity</b>	<b>Timeframe or deadline</b>
Research into topic background. Writing of thesis task.	October 2022 – February 2023
Design and optimization of heatsink	November 2022 – March 2023
Start of compiling the thesis.	January 2023
Submission of thesis task.	21.02.23
Validation/testing of optimized heatsink design at university laboratory.	February 2023 – April 2023
First draft of thesis.	April 2023
Finalizing the thesis.	April 2023 – May 2023
Submission of the final version of the thesis.	18.05.2023
Submission of required defence files.	27.05.23
Defence of thesis.	June 2023

# CONTENTS

ABSTRACT .....	4
LÕPUTÖÖ LÜHIKOKKUVÕTE .....	5
THESIS TASK .....	6
CONTENTS .....	11
PREFACE .....	12
LIST OF ABBREVIATIONS AND SYMBOLS .....	13
INTRODUCTION .....	14
1. LITERATURE REVIEW .....	16
1.1 Drones .....	16
1.1.1 Multicopter design .....	16
1.1.2 Quadcopter motors.....	17
1.2 Heatsink design .....	19
1.3 Topology optimization .....	21
1.3.1 TO in Mechanical design .....	22
1.3.2 TO in Heatsink design .....	24
1.4 Selective laser melting .....	26
1.5 Conclusion of literature review .....	28
1.6 Aims .....	28
2. DESIGN AND OPTIMISATION PROCESS .....	29
2.1 Simulation setup and software .....	29
2.1.1 Software selection .....	29
2.1.2 Model and optimization setup .....	30
2.2 Optimization and simulation results.....	38
2.2.1 Optimized designs .....	38
2.2.2 Simulation results. ....	42
2.2.3 Parameter optimization for comparison .....	47
3. TESTING .....	49
3.1 Manufacturing of the heatsink designs.....	49
3.2 Testing setup and methodology .....	50
3.3 Testing results.....	54
3.4 Suggestions for further development.....	58
SUMMARY .....	59
KOKKUVÕTE .....	61
LIST OF REFERENCES .....	63
APPENDICES .....	67
GRAPHICAL MATERIAL .....	68

## **PREFACE**

The thesis topic was initiated as combination of interests from both the author and faculty members from Tallinn University of Technology (Taltech) School of Engineering. Authors interest in the applications of additive manufacturing was combined with the Universities desires to see if and how they can improve the thermal performance of electrical motors with the use modern design and manufacturing methods.

The completion of this master´s thesis was supervised by Martin Sarap from Taltech. Martin Sarap is an Early Stage Researcher part of the Electrical Machines Research Group under the Department of Electrical Power Engineering and Mechatronics. He provided the author with access to universities manufacturing and testing capabilities required for completing the goals of this thesis.

The author would like to thank his supervisor for the help and feedback provided to him during the different stages of compiling his work.

## **LIST OF ABBREVIATIONS AND SYMBOLS**

Abbreviations and symbols used in this thesis:

AM – Additive Manufacturing

CAD – Computer Aided Design

CFD – Computational Fluid Dynamics

COMSOL – Multiphysics simulation software

MMA – Method of Moving Asymptotes

PBF – Powder Bed Fusion

PO – Parameter Optimization

PSU – Power Supply Unit

SLM- Selective Laser Melting

SIMP – Solid Isotropic Material with Penalization

SLM - Selective Laser Melting

SLS - Selective Laser Sintering

FEM – Finite Element Method

TDP – Thermal Design Power

TO – Topology Optimization

UAV – Unmanned Aerial Vehicle

## **INTRODUCTION**

Nowadays drones have become popular both as hobbyist and professional equipment in different fields. To support their adoption in different applications standardized frameworks [1] have been developed. As these aerial devices/systems have evolved, they have also gotten much smaller while having increased computational and/or electrical power. Small multicopters are especially prevalent in household use or more complex swarm-based solutions.

The small and commonly used coreless DC drone motors, that are also used for Taltech projects, do not have heatsinks. The only heat dissipation element these motors have are the outer metal shells of the motors. Due to the lack of cooling the performance of them is thermally limited. Due to this heatsinks should be used to improve the performance of the drone motors. Lower temperature could also help improve the efficiency of the multicopters as the active power losses will be reduced. This is important as almost all smaller multicopters use batteries as their source of power meaning longer operation time on the same battery capacity.

As heatsinks for drones need to be lightweight and effective then topology optimization (TO) and additive manufacturing (AM) can be ideal technologies to achieve the desired design results. 3D printing, the most common AM technology in use, allows the realization of complex designs gotten from topology optimization. These designs usually resemble organic structures found in nature that are not easily manufacturable with subtractive manufacturing technologies. While existing research on using these technologies together has mostly been centred on optimization of mechanical structures, like in [2], there has been a shift towards other applications, like heatsink design [3][4], only in recent years.

Topology optimization is a set of methods that are used to find an optimal distribution of material inside a specific design space. To find the most optimal results TO is combined with Finite Element Method (FEM) to analyse the parts of the design space in smaller discrete sections. The final state of each element is determined based on the objective function and given design constraints.

The aim of this thesis is to design, manufacture and test optimized heatsinks for a small multicopter motor to improve its thermals and increase its performance. Topology optimization methods will be used in the design process. The optimized heatsink designs will be manufactured with SLM (Selective laser Melting). It allows the manufacturing of metal parts by fusing together layers of metal powder using high-power laser(s). Like

with more common plastic 3D printing it allows for wider design freedom while also making prototyping faster and cheaper.

The main body of this thesis is separated into three main chapters. The first chapter will cover the existing research and solutions related to drones, heatsinks, topology optimization and additive manufacturing that is relevant for achieving the goals of this thesis. The second chapter will describe the design and optimization process used for designing heatsinks for the chosen drone motor. The third and final chapter will describe the testing methodology used to validate the gotten heatsink designs. This chapter will also include the analysis of the aforementioned testing results.

# **1. LITERATURE REVIEW**

## **1.1 Drones**

Most of the small drones related to this work fall under the category of multicopter. These small multi-motor aerial vehicles fit the term of drone [1] by having no human pilots and being operated remotely. Larger aerial drones are usually referred to by the general term UAV (unmanned aerial vehicle) as the design variance is bigger.

### **1.1.1 Multicopter design**

A multicopter design is superior to a helicopter in terms of control and stability due to the dynamics of the multiple propellers [5]. These kind of drone designs have over time evolved better stability and control compared to their predecessor with the help of modern powerful and compact electronics. This stability and the possibilities of accurate control have given these drones a design edge for emerging as an useful platform for both remote-controlled and autonomous applications in different fields [5].

Multicopter designs can vary in the number of motors implemented. This number has big effect on the performance and design constrains for the drone [6]. Larger number of motors means more power, speed, lift capacity etc. but it also comes with its downsides. Each added motor also requires an additional motor control device. With more motor and electronic devices there also comes increased power consumption meaning larger and possible more powerful batteries are needed to feed the devices and keep the required operation time.

In many fields both private and military quadrotor design has become the most prevalent [5][6]. As the name applies these types of drones have four motors. The motors are placed in and X-shape on arms extending out from the main body of the drone. They are mostly placed equal lengths away from each other and the centre of the drone. This gives quadcopters square design. Visual representation of this design can be seen on Figure 1.1. Mostly both the motors and propellers are fixed meaning that the motor body does not turn, and the pitch and other properties of the propeller blades do not change.

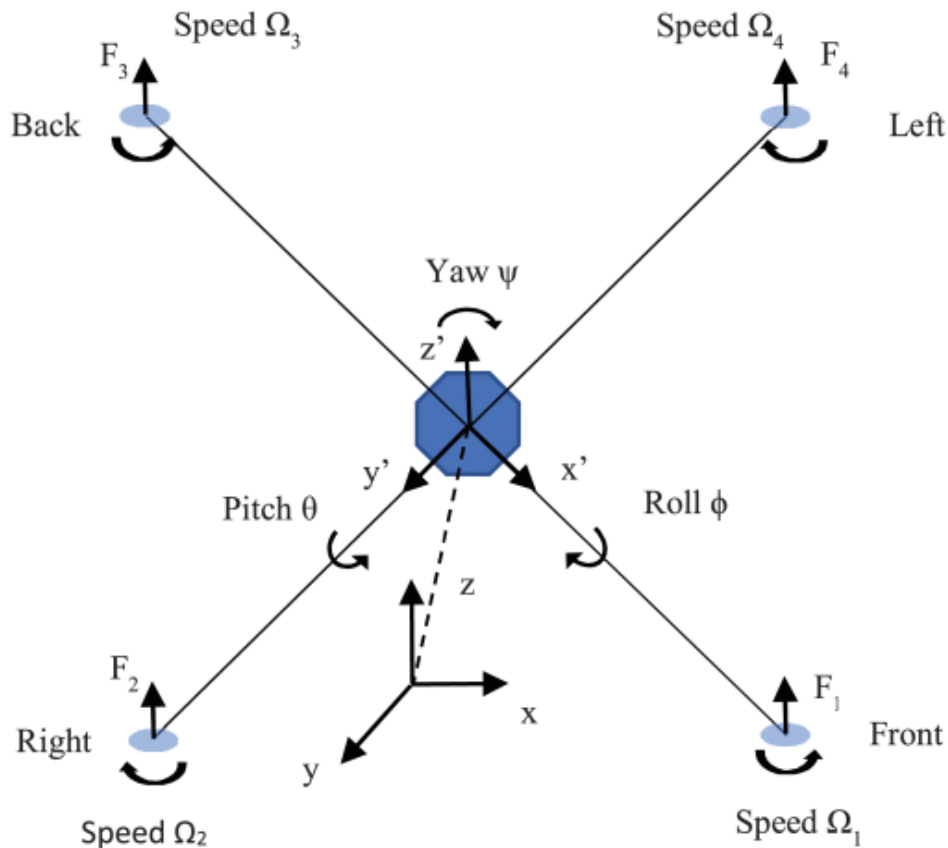


Figure 1.1 Representation of quadrotor drone system [6].

As this type of drone designs are the both the most popular and wide-spread then also the most research is done on or for them. There is number research focusing how the control of the quadcopters can be improved [7][8]. As drones are big part of modern robotics and the goal is to make autonomous machines out of them research is also but into combining them with machine vision [9][10] and finding ways to make multiple of them to be able to work together [10][11].

### 1.1.2 Quadcopter motors

There is a large variety of DC motors available for drones. The specific choice of motor depends on the requirements of the project and the size of the drone. Smaller drones like the DJI Tello, depicted on Figure 1.2, mainly use compact inner rotor motors. In these motors the central shaft of the motor is equipped with windings and rotates inside a stationary enclosure that holds the permanent magnets. These small motors are enough to efficiently move around these small drones that can weigh even under 100 g. DJI Tello, that is very similar to the Taltech drone platform, only ways 80 g [12] for example.



Figure 1.2. DJI Tello drone [12].

Drones used in Taltech projects mainly use 8520 or 1020 size inner rotor coreless DC motors. 8520 size motors are also used for the mentioned DJI Tello. The two first numbers of the motor size describe the diameter of the motor, 8.5 and 10 mm for the mentioned motor sizes. The last two are the length of the motor body, 20 mm for both in this case. Of these two sizes the 8520 is more easily available to buy in separate kits.



Figure 1.3. Picture of 8520 size coreless DC motor [13]. Motor outer diameter is 8,5 mm and main body length 20 mm,

The coreless aspect of these motor comes from the fact that this design does not use iron core like classical DC motors. Instead, a self-supporting cylindrical copper winding in the rotor. The stator is a permanent magnet that fits inside the rotor winding. Internal view of the component making up this type of brushed DC motor can be seen on Figure 1.4. Inner rotor variants of these motors have a separate external housing and the only spinning part of motor that can be directly seen and touched is the rotor shaft.

Coreless motor provides multiple advantage over classical iron core DC motors [14]. Not using iron in the construction reduces mass and rotational inertia of the motor. This means that the motor can change accelerate or deaccelerate faster. Main advantage of this types of motors are that they can achieve higher maximum speeds with the same voltage applied. This is due to them having a lower counter-electromotive force due to smaller changing flux. Coreless motors also have less winding induction meaning reduced electromagnetic interference. The main disadvantages are that they cannot handle transient thermal loads as well because there is no iron core with higher thermal mass to act as a heatsink and low torque.

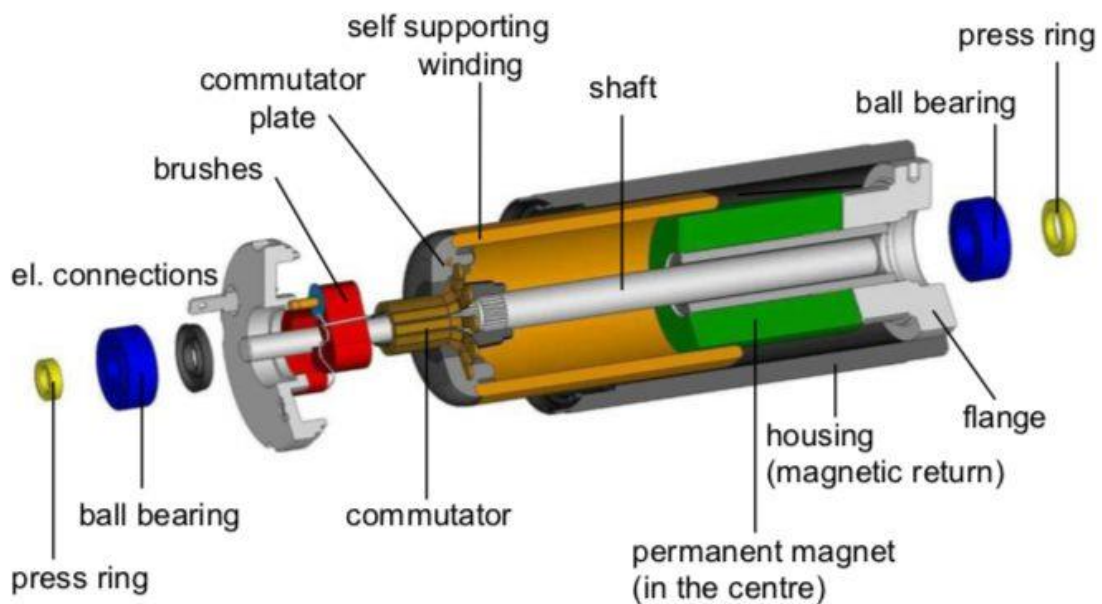


Figure 1.4. Exploded view of coreless DC motor design [14].

## 1.2 Heatsink design

Heatsink design and optimization has historically been a process oriented and focused on different physical parameters [15]. Where parameters like heatsink gauge measurements, base thickness, fin height, fin thickness and number of fins  $N$  are the properties being optimized. Certain limits or restraints are implemented for these parameters during the design process to ensure the manufacturability of the final solution.

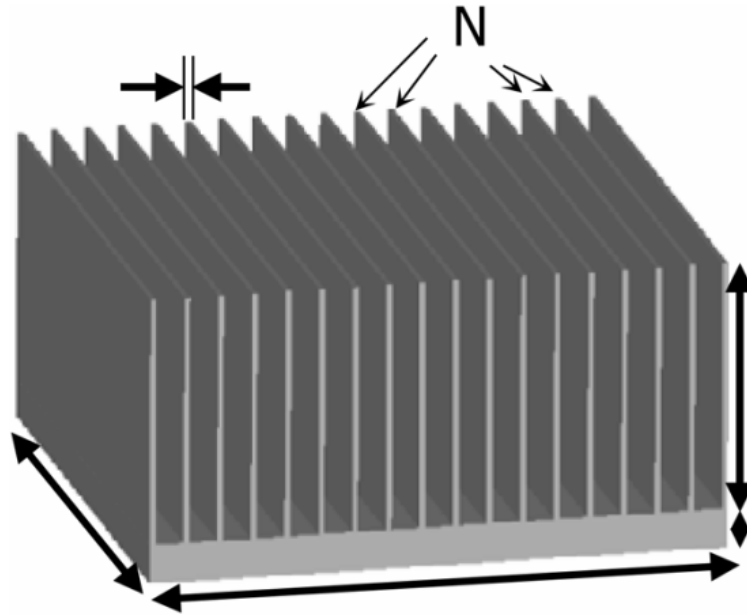


Figure 1.5. Basic parameterised heatsink design [15].

Figure 1.5 shows a common extruded heatsink design where the previously mentioned parameters can be optimised during the design process [15]. As the geometries of these heatsinks are simple then analytical equations exist that can be used for creating the designs. This process is simple and easily configurable with modern software, for example in [16] three different software were used to get the most out of this finned type of design. How and what exactly can be optimized on these designs is constrained by the manufacturing process itself. Most finned heatsinks for air cooling are manufactured by extrusion due to low production cost [16].

The use of modern physics simulations software with spread and increased accessibility of additive manufacturing (AM) has removed many of the shape and topology constraint associated with classical subtractive and extrusion manufacturing [16][17]. This enables the use and realization of more advanced parameter optimization [16], geometry optimization [15], generative and topology optimization. Based on the project requirements these methods can be combined to achieve the most optimal results. Many simulation programs have evolved from just simulation environments to having tools to use the mentioned methods to generate parts or objects based on the information they are able to generate about physical phenomena and rules. All of these methods can produce complex designs that are impractical to be manufacture with classical methods but are not a problem for additive manufacturing like selective laser melting (SLM).

If software heatsink optimizations problems are mostly solved as standard nonlinear optimization problems that are in the following the instruction set (1.1) [3].

$$\begin{aligned}
& \text{minimization of } f_0(x) \\
& \text{subject to } f_i \leq 0 \\
& \quad i = 1, \dots, m \\
& \quad j = 1, \dots, n \\
& \quad x_j^{\min} \leq x_j \leq x_j^{\max}
\end{aligned} \tag{1.1}$$

Where

- $f_0$  – the objective function that optimization process aims to minimize,
- $f_i$  – represents the systems behaviour constraints,
- $m$  – the number of constraints,
- $n$  – vector of  $x_j$  design variables.

Heat transfer problems are solved for the governing equation of conservation of energy. In steady state the heat transfer is represented by Fourier's law, formula (1.2) [3].

$$Q = -\nabla \cdot (k \cdot \nabla T) \tag{1.2}$$

Where

- $Q$  – volumetric heat generation, W,
- $k$  – thermal conductivity of the material, W/(m·K),
- $\nabla T$  – temperature gradient, K/m,

## 1.3 Topology optimization

The field of Topology optimization (TO) was first pioneered by Martin P Bendsøe and Ole Sigmund who covered the topic in detail in their book "*Topology Optimization: Theory Methods and Applications*" [3][18]. Who mainly focused on the methods applications for structural engineering. Their researcher based on the Density method optimization has been coupled with the Method of Moving Asymptotes (MMA) [4][19] optimizer and then been used as the basis for many of the subsequent research on the topic. The application of their combined approach without regularizations or constraints will lead to vague domain determinations. This means that there can be inaccurate due to material boundary being defined as partially fluid and partially solid at the same time.

TO is a mathematical approach for achieving optimal distribution of material inside a certain defined design space [20]. To be able to achieve the optimal results with TO Finite Element Method (FEM) is applied at the same time. FEM can be both used for analysing the performance of existing and new optimized designs while also being a tool for the development process. In FEM to analysis how some physical phenomena affects an object it is divided into smaller finite elements that can be assessed separately during the simulation. The set of the finite elements is usually called a mesh. The finer the

mesh the more accurate the result will be but it will come at the cost of increased computational power or time being required. This division of objects into a mesh allows the analysis and determination of optimal material distribution for TO problems.

The distribution of material is determined based on the objective function and clearly defined constraints. This is done using a design variable  $\theta$  (theta) that gives each finite element a density value between 0 and 1 [3]. Element with value 0 means that an element is either empty or is filled with a fluid, this depends on the problem being solved, and value of 1 shows that a certain element should be solid. To direct the design elements value to certain edge of the range a penalization scheme is used. One of the most common being schemes applied is Solid Isotropic Material with Penalization (SIMP). The element material properties are determined by using the following formula (1.3) [3].

$$x_{SIMP} = (x_{max} - x_{min}) \cdot \theta^n + x_{min} \quad (1.3)$$

Where

- $x$  – certain property of the material (for example thermal conductivity),
- $x_{max}$  – maximum possible value for the material property when it is a solid,
- $x_{min}$  – minimum possible value for the material property,
- $\theta$  – design variable that ranges between 0 and 1,
- $n$  – penalization factor that determines penalization curve that shows how much the design variable will be penalized for not being equal to 1,
- $x_{SIMP}$  – value of the material property based on the SIMP scheme.

While its main application is still predominantly in the field of structural mechanics it has also been becoming increasingly more popular and adopted in other diverse areas. [4] This is due to it being usable and flexible for solving many optimization problems involving different physics problems. It works in steps advancing towards a final optimal design in an iterative manner.

### **1.3.1 TO in Mechanical design**

As mentioned before, the main application for TO is mechanical and structural design in different fields. The main factors motivating its use being possibility of achieving reduced weight and increased strength of parts or assemblies. These are important properties for designing products and machines for industries like aerospace, aviation and automotive.

For aerospace applications researchers [21] used topology optimization to create a new lightweight thruster bracket design for attaching thrusters do the satellite board. The main important performance aspect being the bracket ability to resist deformation caused by launch process. TO was used by the researchers in the optimization process for this bracket as it provides a reasonable structure shape according to user specified boundary and loading conditions.

Although TO could not accurately determine the needed structure, optimization process result can be seen on Figure 1.6, it gave researchers [21] ideas and indicated directions where the overall structure design should go. Improved understanding of the product was used to create 3D printable rod structure suitable as the bracket, shown on Figure 1.7. The bracket design was verified using software analyse.

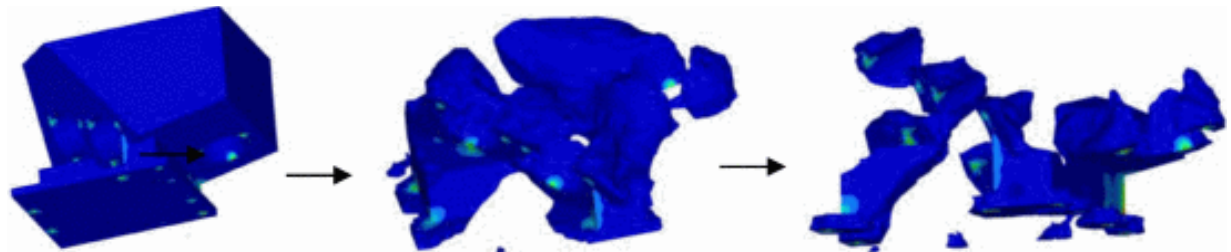


Figure 1.6. Optimization process of the thruster bracket. [21]

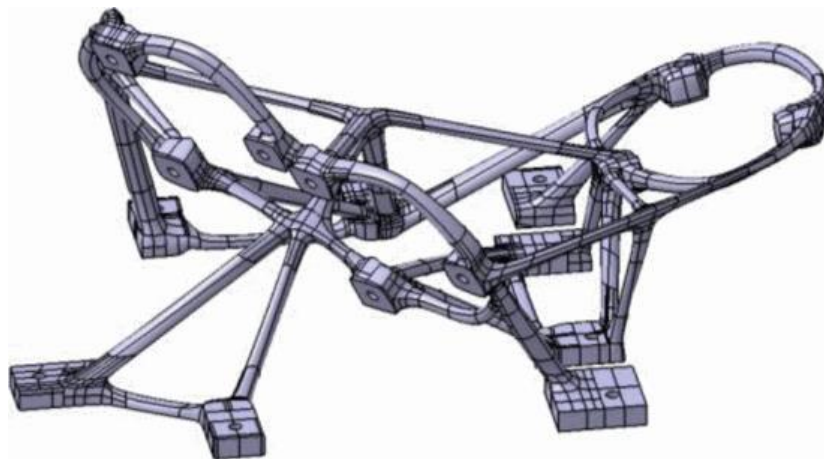


Figure 1.7. Final thruster bracket design.[21]

Similar design optimization process has also been used for aviation. This kind of approach can be especially beneficial for new planes where lighter and stronger structures are able to improve flight range, maximum altitude, endurance, flight speed while also reducing fuel consumption and emissions. Study [22] focused on the optimization of aluminium air brake bracing beam for L-39ZA military airplane. The aim of the study was to reduce the weight of the bracket using TO in ANSYS Workbench.

### 1.3.2 TO in Heatsink design

As mentioned before heatsink design is another emerging use case for topology optimization. The main driving force behind it again being the advent of additive manufacturing that removes the constraints heatsink manufacturing methods such as extrusion and casting impose on the design possibilities. In [23] authors of the work explored a heatsink design process that uses the iterative topology optimization process to generate the design.

Like with optimizing mechanical design the process tried to find the optimal distribution of material inside a given design space. Instead of the aims being the reduction of mass while improving the structural strength the aim of the researchers works [23] was to improve the thermal performance of the heatsink by focusing on thermal compliance. Thermal compliance referring to how easily a bodies temperature changes when a thermal load is applied to it.

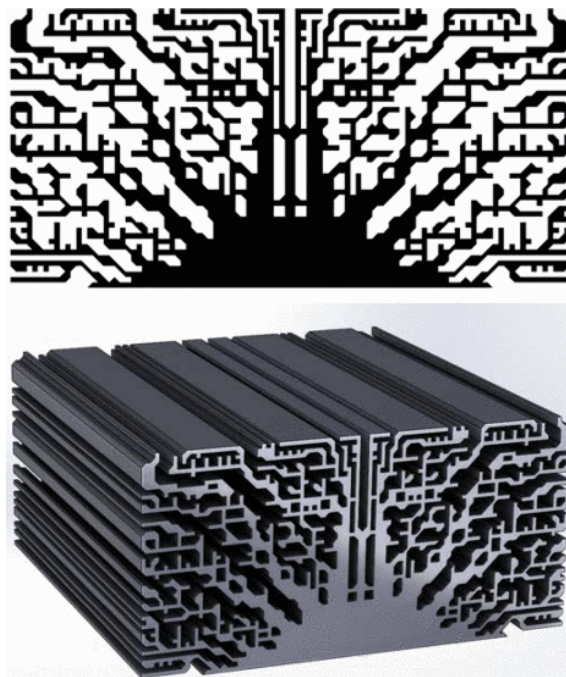


Figure 1.8. 2D and 3D perspective of the final gotten designs. [23]

The process was applied to a 2D cross-section profile of a forced convection cooled heatsink. Even though their result from topology optimization was not significantly better than from parametrically optimized finned design they considered it as good starting point for refining the optimization process and trying it in 3D space. The final gotten heatsink design can be seen on Figure 1.10 where its also shown as 3D object.

Although advancements have been made in thermal topology optimization many challenges remain. In [24] it is discussed the main challenge being modelling of heat transfer in convection solutions. The core of the problem being in the boundary layers of the heatsink where state of the finite elements can be uncertain. In that layer the solutions for both heat transfer and fluid flow can dominate over the main optimization function. This process is already computationally intensive and complex for laminar flow solution meaning that even greater problems are with the use of turbulent flow dynamics in this process. Progress has been made how to apply these methods but computational resource requirements for solving each iteration are still high especially for solutions solved for three-dimensional space.

As Computational Fluid Dynamics (CFD) usually brings more issues than advantages to TO of heatsink then it is mainly used for validation or modelling of the thermal solution. Most studies on TO implement, like [25], the optimization process itself is conducted in 2D space using convection coefficients to save on computational power needed and calculation time. 3D simulation space was used to validate the optimized natural convection heatsink designs. Validation process showed that the new design should achieve a lower average temperature of about 16 °C and the performance comparison can be seen on Figure 1.11.

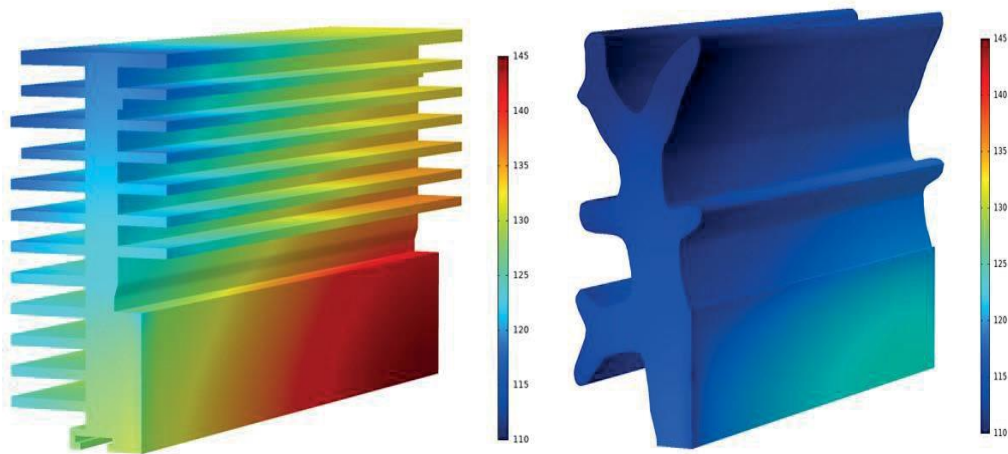


Figure 1.9. Initial heatsink design (left) vs TO improved design (right). [25]

Use of CFD is more reasonable for parametric optimization like in [26] where it was used for numerical development of five different novel heatsink designs. These designs featured ribs, grooves, and fins generated through different parameterized formulas.

In [25] it was also proposed that after the initial optimization process the design work could be expanded on and refined by fractal approach mimicking nature. This meant that base geometry gotten from the initial TO was repeated for each main and sub-

branch. After that the design should be trimmed to respect the constraints applied to the design space. This process is visualized on Figure 1.12.

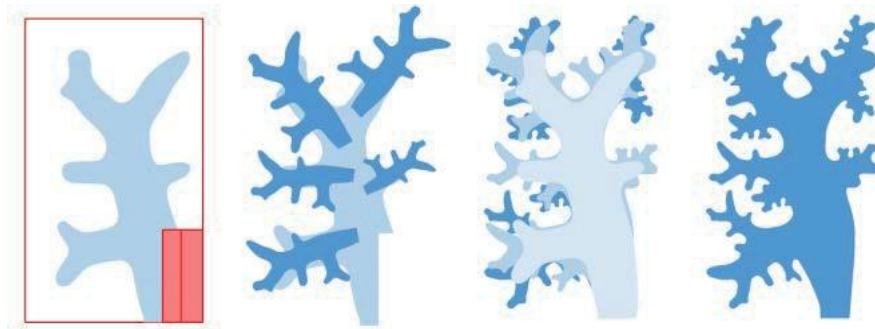


Figure 1.10. Fractal approach to evolve the heatsink design. [25]

This fractal bioinspired method was suggested because TO was limited regarding the smallest features it could produce. This was due to mesh refinement and the computational resources available. As mentioned before, smaller elements in the mesh will lead to higher need of computational power to complete the calculations in a reasonable amount of time.

## 1.4 Selective laser melting

From different research and studies, it's clear that maturity of additive manufacturing technologies is one of the driving forces behind the adoption of TO for design and development of parts. 3D printing allows the realization of design too complex for more classical subtractive manufacturing methods.

As prevailing amount of heatsink are made of metal then AM technology capable of printing metal materials needs to be used. Selective Laser Melting (SLM) is variant of Powder Bed Fusion (PBF) capable of manufacturing 3D metal parts additively from various reactive and non-reactive metal powders [27]. The metal parts are created by melting together thin layers of heated up powder material. Laser scanning is used to apply 2D geometries that are derived from the 3D designs on to each layer while also combining this geometry with one on the previous layer. The bonding of the powder particles for these geometry layers is affected by laser velocity, laser scan speed, scan strategy, chamber temperature, powder temperature and how exactly powder is applied.

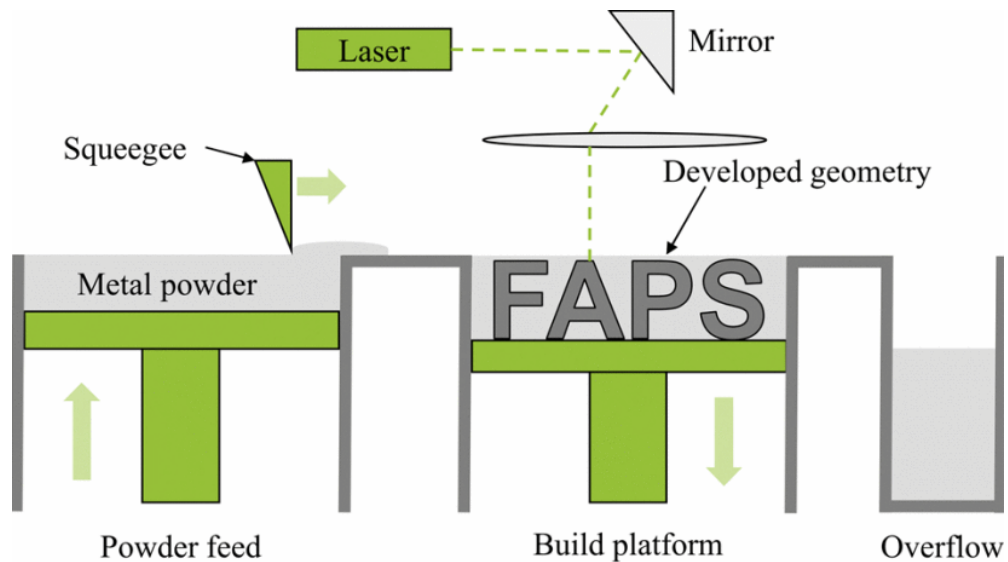


Figure 1.11. Basic structure of SLM 3D printer. [27]

Figure 1.13. depicts the common two chamber set-up of SLM printer. First chamber is the feed chamber that is filled with the metal powder at start of printing process. Heated powder from the first chamber is applied to the second chambers build platform as thin layer. Then the geometry is apply using the laser. For adding the next build layer base of the feed chamber moves up to reveal new material while the build platform lowers itself to be ready for receiving the next layer. Additional overflow chamber is used to capture excess material from when it is applied to the build surface. This type of printer configuration is also used for other types of materials use with SLS technologies.

Aluminium based materials are mostly used for SLM printing parts for thermal applications. For example, in [28] where it was studied how different printing parameters like laser power and scanning speed affect mechanical properties of parts printed from AlNiCo magnetic material. Additionally, use of material like titanium, steel, ceramics etc with SLM has also been researched. Work has also been but in how to best print copper materials [29]. Widely used infrared lasers used in SLM printers are not well suited for printing pure copper.

## **1.5 Conclusion of literature review**

From different sources of literature, it could be clearly seen that even though concepts behind topology optimization have already existed for few decades the real usability and feasibility of this approach have been increased by advances in manufacturing technologies and increased computational power available during the last decade. Additive manufacturing allows the realization of designs not possible before. Modern computational power speeds up the generation of more precise topology optimized solutions while also offering possibilities of better visualization both in 2D and 3D dimensional simulated space.

While existing research in this field has historically been more focused on solutions for structural problems there has been an uptake in its adoption for other applications as well. For example, tries have made to find improvements in designs of electrical devices and heatsinks. Heatsink design with topology optimization being the slightly newer and less explored direction for research.

As topology optimization has been already seen to be potentially feasible solution for improving mechanical parts from aviation it could also be realized for drones that follow most of the same principles as actual aircraft but just on a smaller scale. Use of topology optimization can create custom light-weight heatsinks designs for drone motors. Small motors which thermals are usually not well management. Better thermals can lead to better motor performance while also might having other positive effects on the drone as and whole system.

## **1.6 Aims**

The aims for this thesis work are:

- Design an optimized heatsink for a small drone motor.
- Use topology optimization in the design process.
- Test the optimized designs in the simulation software, COMSOL.
- Manufacture the heatsink(s) using additive manufacturing SLM.
- Testing of the heatsink designs in real environment.

## **2. DESIGN AND OPTIMISATION PROCESS**

### **2.1 Simulation setup and software**

#### **2.1.1 Software selection**

COMSOL Multiphysics Simulation Software [30] was chosen as the design and analysis tool as it provides multiphysics and single-physics modelling capabilities for a variety of physics phenomena. The software's model and application builders implement all the necessary tools needed for a complete workflow of physics modelling for different fields of engineering, manufacturing, and scientific research. Version 6.0 of COMSOL was used to complete the task of this thesis work.

The software includes computer aided design (CAD) tools that can be used to create the geometries of the parts being analysed and/or optimized. Material properties of parts can be configured in detail. Effects of electromagnetics, structural mechanics, acoustics, fluid flow, heat transfer, and chemical reaction phenomena can be simulated in one software. COMSOL also includes an optimization module that includes tools for parameter, shape and topology optimization.

COMSOL's website has a wide variety of tutorials and examples available of how different physics phenomena and optimization methods can be modelled in the software environment. Like for example [31] that gives an introduction to how to model and simulate heat transfer and fluid flow for evaluating heatsink performance. There is also a variety of other examples showing how to apply the optimization tool for part design. These mainly cover applications related to structural design and fluid flow.

Model building and simulation can be performed both in 2D and 3D space depending on the user's needs and requirements. 0D and 1D space dimensioning is also available but those are not relevant for this thesis work.

For additional CAD design and modifications of the optimized heatsink designs Autodesk Fusion 360 3D modelling software was used. It was used as it offers more flexible design tools than COMSOL and the author of the thesis work also has previous experience with it.

## 2.1.2 Model and optimization setup

The drone heatsink model was created in 2D space as it provides a simpler and less computationally intense way to complete desired design objective of heatsinks topology optimization. 2D solution also makes it easier to avoid issues that can rise from solving active cooling CFD and TO problems at the same time. In 2D fluid flow can be approximated using convective heat flux. 3D optimization process is more suitable for passively cooled solutions where the air flow is due to natural convection of heat and not actively generated. 2D solution allows for more reasonable computational time without extreme computational power due to having 2D mesh with significantly fewer finite elements than the same density mesh would have if it was created in 3D. This means that 2D mesh can be a lot finer resulting in better accuracy for the achieved solution without long computational times. Also, the motor and propeller used in this work are able to generate uniform and stable airflow that can be approximated well in the 2D designs space.

For the optimization process then a 2D model with the required heat transfer module was created. As there is no direct simulation of air flow during the TO process then physics module covering only heat transfer in solids was used. This module allows the active air flow to be considered as forced convective heat flux. The created COMSOL solution set up is based on instructional videos [32] and [33]. These videos reflect and apply the methods and principles that were used in [3]. Different values required were parameterized with units relating to them. The use parameters allowed the model to be more easily changeable and trackable as the values could be changed from one place instead needing to change them inside different software function settings.

### 2.1.2.1 Geometry creation

2D space allowed the geometry used for TO to be very simple. Heatsink and motor design space could be represented by just creating two circles. Inner one representing the motor and the outer one the allowed space for the heatsink. This geometry was created with parameters brought out in Table 2.1. Motor measurements stayed the same but heatsink outer diameter was changed to develop different designs. Motor height would be later required to define the heat flux from the airflow.

Table 2.1. Motor and heatsink parameters with used values.

Parameter	Value	Unit	Description
D_motor	8,5	mm	Motor diameter
H_motor	20	mm	Motor body height
D_heatsink	12 - 25	mm	Heatsink outer diameter

### 2.1.2.2 Defining materials

Materials used needed to be defined for both the motor and heatsink design space domains. Even though the motor is made of multiple materials for the simulation it was simplified to be cylinder made of 4310 Steel that has thermal conductivity over 3 times lower than the aluminium alloy, properties shown in Table 2.2, used for the heatsink. In COMSOL this built-in steel alloy has thermal conductivity of 44,5 W/(m·K). Lower conductivity material was used as the exact thermal properties of the motor are unknown.

As the exact material distribution of the heatsinks design space is determined by TO then the exact material properties of each finite element are determined by the Solid Isotropic Material with Penalization (SIMP) scheme. This means that blank material needs to be created where the properties are calculated following the SIMP formula explained in subchapter 1.3. The finite element properties could either gravitate towards being made of air or the A360 (AlSi10Mg) aluminium alloy.

Design spaces density was calculated as:

$$\rho_{SIMP} = (\rho_{solid} - \rho_{air}) \cdot \theta^n + \rho_{air} \quad (2.1)$$

Thermal conductivity as:

$$k_{SIMP} = (k_{solid} - k_{air}) \cdot \theta^n + k_{air} \quad (2.2)$$

Specific heat capacity as:

$$Cp_{SIMP} = (Cp_{solid} - Cp_{air}) \cdot \theta^n + Cp_{air} \quad (2.3)$$

Where

$\rho$  (*rho*) – material density, kg/m<sup>3</sup>

$k$  – thermal conductivity, W/(m·K),

$Cp$  – specific heat capacity, J/(kg·K),

$\theta$  – design variable that ranges between 0 and 1.

$n$  – penalization factor.

The values that were used for the material properties are defined in Table 2.2. Solid in parameter name refers to the aluminium alloy that is used for metal 3D printing. Formulas (2.1), (2.2) and (2.3) were used as the properties of the design space material. These material property values were taken from [34].

Table 2.2. Values used for material properties.

Parameter	Value	Unit
rho_solid	2700	kg/m <sup>3</sup>
k_solid	150	W/(m·K)
Cp_solid	1060	J/(kg·K)
rho_air	1,205	kg/m <sup>3</sup>
k_air	0,1	W/(m·K)
Cp_air	0,1	J/(kg·K)

### 2.1.2.3 Configuration and creation of mesh

As solving the TO objective requires the use of FEM then finite element mesh needed to be created from the geometry. In COMSOL mesh can be created either automatically based on the physics and generalized mesh size or the process is user defined. To have more control over mesh creation and take SLM manufacturing restrictions into account, like in [3], then it was done with the help of user defined parameters.

Table 2.3. Used user controlled mesh parameters.

Parameter	Value	Unit
hmax_design	0,1	mm
hmax_solid	0,2	mm

Parameters shown in Table 2.3 limit the size of the elements created in either the design or motor domain. Parameter referring to solid is for the motor domain where the mesh can be less dense as the material properties stay the same during TO process. Less dense mess also helps to reduce the computational time. Finer mesh for the design space helps to achieve a more accurate simulation result and a better optimized geometry. Triangular mesh created, that adheres to these size constraints, can be seen on Figure 2.1. The TO filter radius was set to 0,4 mm to block the creation of design features too small to be manufactured. This was configured inside the TO physics tool of COMSOL.

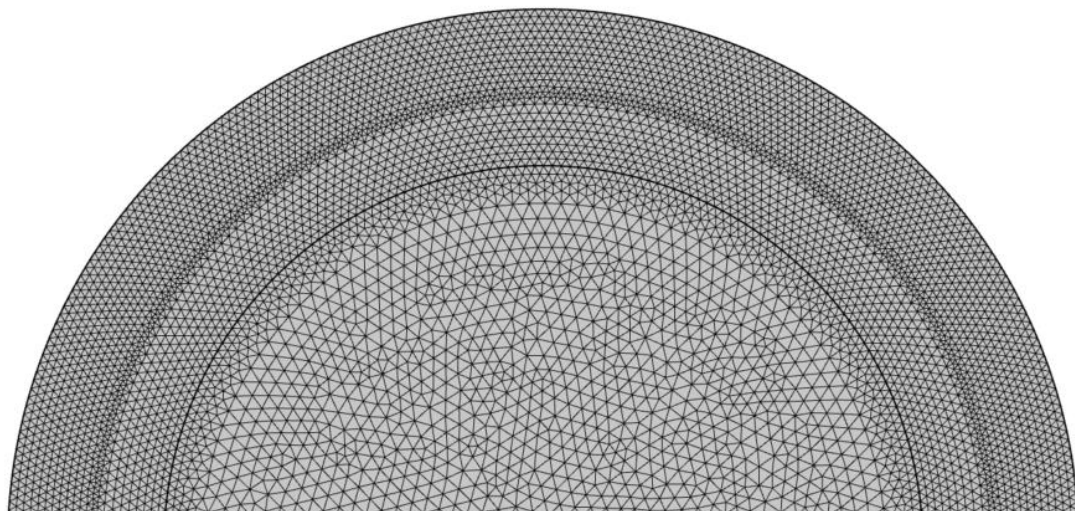


Figure 2.1. Top half of user controlled mesh created for motor with 12 mm diameter heatsink.

#### 2.1.2.4 Physics configuration

As mentioned before for topology optimization *Heat Transfer in Solids (ht)* built-in software physics module of COMSOL was used. This module provided the necessary framework to simulate the heat transfer from the motor to the heatsink.

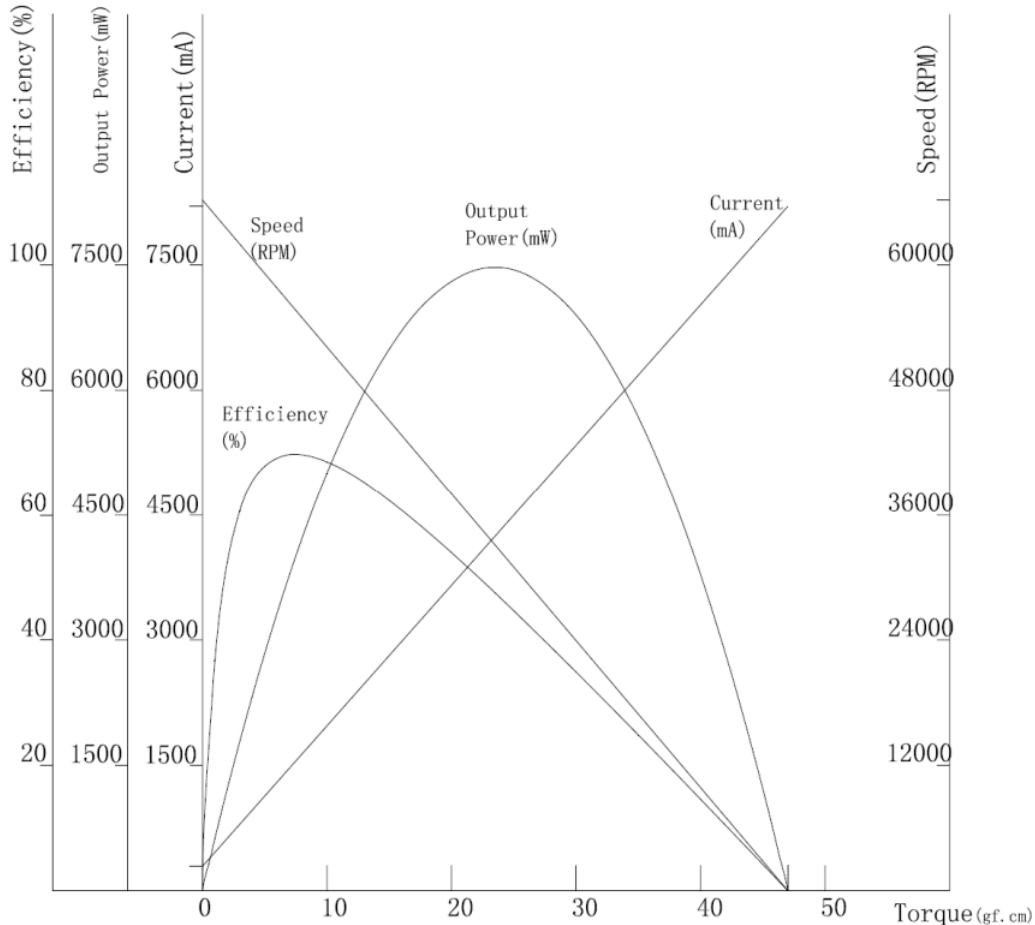


Figure 2.2. Ineed 8520 motor electrical performance curves. [35]

Motor domain of the geometry was configured to be the Heat Source. There are variety of manufacturers for the 8520 size motors and most of them do not have any performance and efficiency data available for the motors they produce. Only manufacturer that author of this work found with this information available was Ineed Electronics. Performance and efficiency information was available for their IND - YQ8520 - 001 motor [36].

From the motors electrical performance curves on Figure 2.2 it may seem that these motors are inefficient but IE electric motors efficiency class standard IEC 60034 [37] demonstrates otherwise. While the standard does not go as low as the used drone motor in terms of power range it clearly shows that less powerful motors can be considered to be efficient at much lower efficiencies than the more powerful electric motors. According

to the manufacturer's datasheet at max output power of about 7,5 W the efficiency is 47,5 %. The motor is the most efficient at 69,7 % when output power is 4 W. From this information the thermal losses of the motor could be calculated. The losses mainly come from active power losses in the windings. Minor part of the losses are due to mechanical friction and eddy currents in the motor outer shell and permanent magnet. Losses can be calculated with following formula (2.4).

$$P_{losses} = \frac{P_{output} \cdot 100}{\eta} - P_{output} \quad (2.4)$$

Where:

- $P_{losses}$  - are the losses generated by the motor in W.
- $P_{output}$  - mechanical output power from the motor in W.
- $\eta$  - efficiency of the motor in percentage.

When motor is run at maximum power the losses are:

$$P_{losses} = \frac{7,5 \cdot 100}{47,5 \%} - 7,5 \approx 8,4 \text{ W}$$

And at maximum efficient the losses are:

$$P_{losses} = \frac{4 \cdot 100}{69,7 \%} - 4 \approx 4,6 \text{ W}$$

To account for situations where the motor needs to be ran at maximum power for a longer period time the motor was configured to heat source with constant heat rate of 8,4 W. This also helps to take into account the fact that most these motors are of Chinese origin and the exact quality and efficiency of these motors are unknown and untested.

The design domain around the motor was set up as the heatsink. It was configured to be a heat source with negative heat rate of -4,2 W. Setting a negative heat rate for the design domain is not mandatory for the optimization to work but most COMSOL examples used it to encourage the heat transfer between the two solids so that the heat would be encouraged to flow away from the motor into the outer regions of the heatsinks. This gives the heatsinks some kind of initial thermal design power (TDP) to aim at and encourages branching in the heatsink design. Like in the instructional videos this value was set to 50 % of the thermal losses.

The air flow created by the propeller attached to the drone motor was applied as forced convective heat flux to the outer edge of the design space. Configuration for this heat flux allowed also to take into account the height of the motor and heatsink as length of the plate that the air flow passes. Velocity of the air movement was calculated as measuring it would not be reasonable or realistic. Air velocity was calculated with formula derived from the propeller thrust formula (2.5) [38]:

$$F = 0,5 \cdot \varphi \cdot A \cdot (V_e^2 - V_0^2) \quad (2.5)$$

Where

$A$  – area the propeller blades pass through while moving,  $m^2$

$F$ - force/thrust, N.

$V_e$  – exiting airflow from the propeller, m/s.

$V_0$  – free airflow, m/s

$\varphi$  – air density,  $kg/m^3$

The derived formula (2.6) for generated air velocity is:

$$V_e = \sqrt{\frac{F}{0,5 \cdot \varphi \cdot A} + V_0^2} \quad (2.6)$$

Assisted by the flowing two formulas:

$$F_{floating} = m \cdot g \quad (2.7)$$

$$A = r^2 \cdot \pi \quad (2.8)$$

Where

$m$ - mass of the object being propelled, kg.

$g$ - gravitational constant, 9,81 N/kg

$r$  – radius of the propeller, m.

As mentioned before, the drone used by Taltech is similar to the DJI Tello that weights 80 g and uses propellers with a diameter of 76 mm. Drone has four motors meaning the weight they are required to lift is divided. The mass for one of the optimized heatsinks is estimated to be 5 g and needs to be taken in to account as well. This means each of the four motor needs to equally lift about 25 g of mass Velocity of the free airflow is considered to be equal to 0. This represents an ideal case where the free air that the propeller will pull in is completely still. Using this information, the air velocity required to keep the drone floating could be calculated as follows:

$$V_e = \sqrt{\frac{0,025 \text{ kg} \cdot 9,81 \text{ N/kg}}{0,5 \cdot 1,205 \text{ kg/m}^3 \cdot (0,038 \text{ m})^2 \cdot \pi}} + 0^2 = \sqrt{\frac{0,1952}{0,00273}} \approx 9,14 \text{ m/s}$$

### 2.1.2.5 TO configuration

The final step of setting up the simulation model was to configure the topology optimization. This required choosing of the optimizer and defining the objective function with suitable constrains. For optimization solver Method of Moving Asymptotes (MMA) was selected. The sources in Literature Review chapter cover it to be the most common optimizer for TO and COMSOL uses it by default. The objective function was compiled based on the Fourier's law and an additional penalty term to filter out elements intermediate density like was done in [3]. This penalty term needs to be considered, so the optimization process also considers the manufacturing restrictions. Without this penalization features may be created that are too small to be manufactured with SLM.

Part of the objective function coming from Fourier's law is represented by formula (2.9) [3].

$$f_{0,1} = \int_{\Omega} k_{simp} \cdot (\nabla T)^2 d\Omega \quad (2.9)$$

The square seems to be added for increasing the functions sensitivity to changes in temperature gradients values. From testing the objective function, it was seen that the optimization process does not work without it. With it removed the optimization just produces a circular material distribution.

Penalty term part of the functions being formula (2.10) [3].

$$f_{0,2} = \int_{\Omega} |\nabla \theta|^2 d\Omega \quad (2.10)$$

While the source [3] also includes an extra part to the penalty term to implement manufacturing restrictions it can be left out without disturbing the optimization process significantly. The same restrictions can be easily and successfully implemented just by manually changing the mesh size to fit the smallest size detail manufacturing process or device can produce.

Combination of formulas (2.9) and (2.10) with weighing between the objectives being gives the formula (2.11) for the final TO objective function.

$$f_0 = (1 - q) \cdot \int_{\Omega} k_{simp} \cdot (\nabla T)^2 d\Omega - q \cdot \int_{\Omega} |\nabla \theta|^2 d\Omega \quad (2.11)$$

Where:

$f_0$  – objective function,

$q$  – weighing factor between the objectives,

$k_{simp}$  – thermal conductivity of the finite element, W/(m·K)

$\nabla T$  – temperature gradient, K/m,

$\nabla \theta$  – design variable gradient.

Do avoid a situation where design space is 100 % full of material as the result of TO the average material volume factor ( $\gamma$ ) was used as a constraint. Its upper limit was set below 1 to control what percentage of design space finite elements can be defined to be solid material.

## 2.2 Optimization and simulation results

### 2.2.1 Optimized designs

14 different topology optimized heatsink design with variety of values for heatsink outer diameters and upper bounds for the average volume factor were created for real world testing. 3 of the created heatsink designs were created to be square instead of circular. This was done out of interest to see what will be the TO results with different shape design space and how their performance compares to circular heatsinks.

Table 2.4. Variants of circular heatsinks.

<b>Diameter [mm]</b>	<b>Maximum average volume factor</b>
12	0,5
15	0,35
15	0,5
15	0,65
20	0,35
20	0,5
20	0,65
25	0,35
25	0,5
25	0,65

Table 2.5. Variants of square heatsinks.

<b>Square side length [mm]</b>	<b>Maximum average volume factor</b>
12	0,5
15	0,5
20	0,5
25	0,5

Multiple other simulations were run to see how exactly changing of different parameters affect the TO results. From these simulations it could be seen that changing the value of air velocity, objective weighing factor did not significantly affect the optimization results. On the other hand, finite element size and allowed maximum average material volume factor had larger impact on how the heatsink design developed.

Each topology optimization was run for 100 iterations. For the used mesh sizes this was enough to reach a result where further iteration would significantly change the gotten results. Even running 1000 iterations did not alter the result but significantly increased the computational time. Additional iterations were impactful if the mesh size would to be reduced. With less fine of a mesh the extra iterations allowed TO produce results closer to the ones that were ran with denser mesh. As previously mentioned, the size of the mesh generated for the TO was determined by the two parameters shown in Table 2.3.

Topology optimization process generated relatively symmetrical, and uniform heatsink designs. Where the so called branches of the heatsink were created in a quite exact circular pattern. From Figures 2.3, 2.4, 2.5 and 2.6 the increased branching, allowed by the increase of heatsink design space diameter, can be seen for the same allowed average material factor. This increased branching could happen as the increased diameter meant more material meaning also more finite elements the TO could work with to achieve the most optimal design. Most of the branching occurred in the outer regions of the heatsinks. The TO material distribution generated smaller design details in the outer regions of the design space.

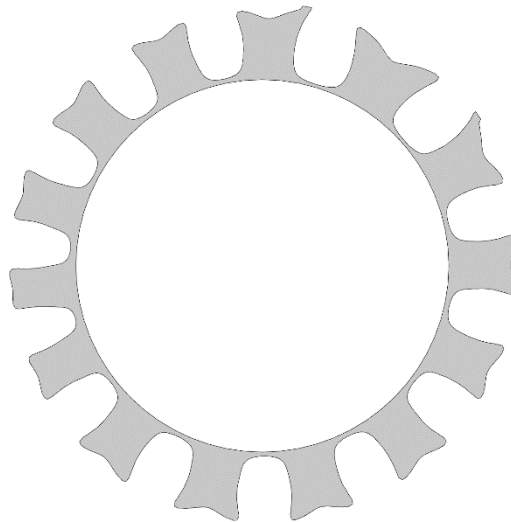


Figure 2.3. TO design with diameter of 12 mm and average material factor of 0,5.

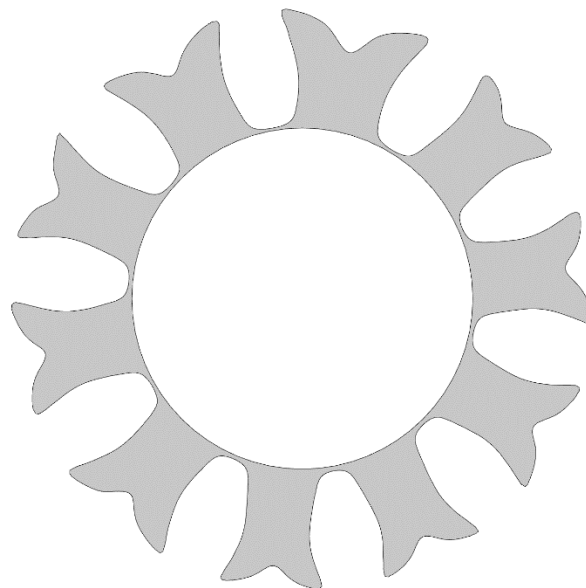


Figure 2.4. TO design with diameter of 15 mm and average material factor of 0,5.

While the differences between designs with diameters of 12, 15 and 20 mm is significant and noticeable the design development slowed after this point. The 25 mm diameter heatsink design, shown on Figure 2.6, is similar to a step smaller heatsink design. The main visible difference being longer branches that do not diverge into smaller ones further. This decrease in divergence was caused by the TO filter radius that did not allow the design features get smaller.

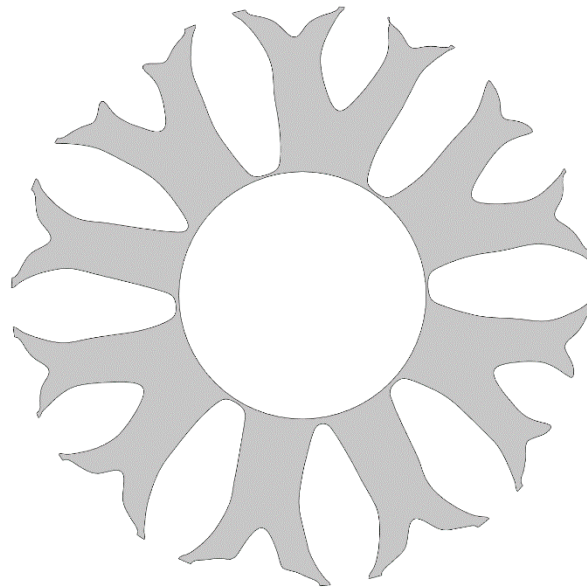


Figure 2.5. TO design with diameter of 20 mm and average material factor of 0,5.

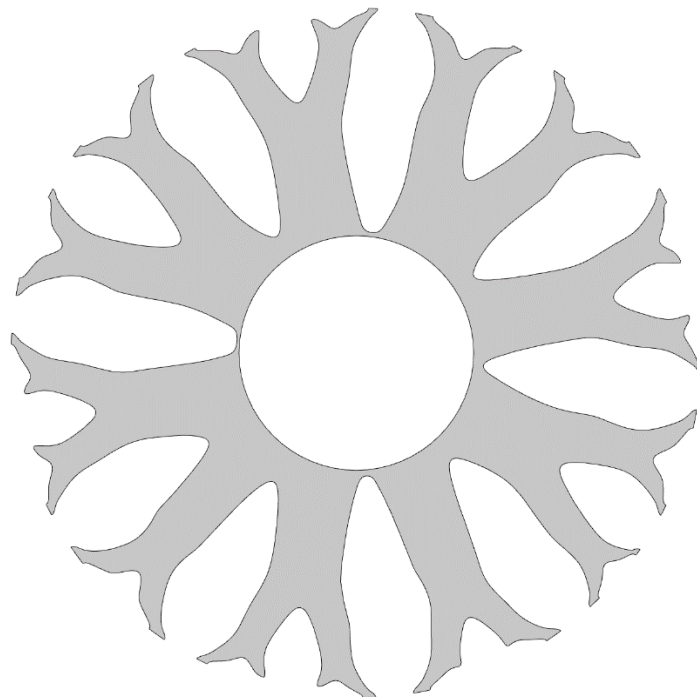


Figure 2.6. TO design with diameter of 25 mm and average material factor of 0,5.

While the designs gotten with maximum average volume factor of 0,5 mm led to symmetric and orderly designs decreasing it resulted in irregular designs. For example, on Figure 2.7 the 20 mm heatsink can be seen with material factor reduced to 0,35. This design is much more erratic and inconsistent compared to the one shown on the Figure 2.5. This was true for all the heatsink diameter sizes.

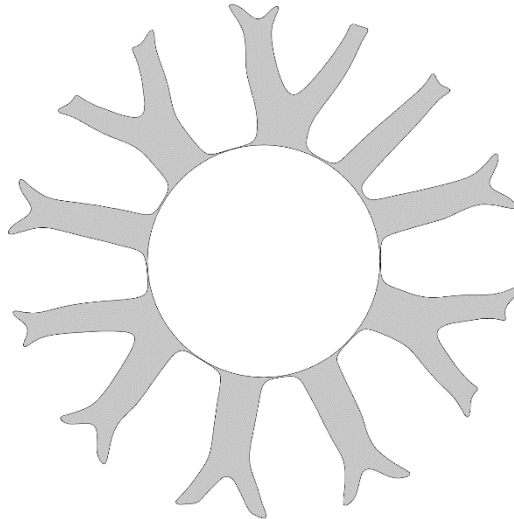


Figure 2.7. TO design with diameter of 20 mm and average material factor of 0,35.

On the other hand, increasing the average material volume factor gave similar designs just with the branches of the heatsinks being visible thicker. Example of this can be seen of Figure 2.8. where volume factor was increased to 0,65. Even if this added thickness increases performance it will also increase the weight what is not ideal for drones.

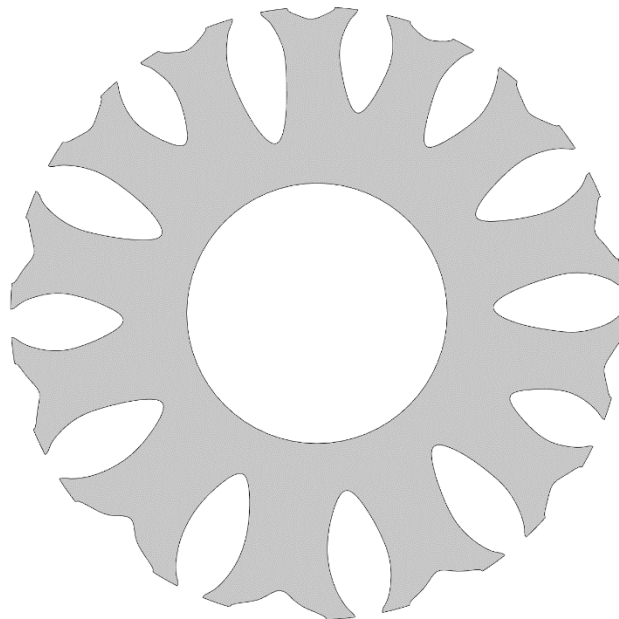


Figure 2.8. TO design with diameter of 20 mm and average material factor of 0,65.

Similarly, to 20mm diameter radial heatsink with volume factor of 0,5 the square heatsink design achieved was rather symmetrical and uniform. An example of how TO generates an optimized heatsink design for a square space can be seen on Figure 2.9.

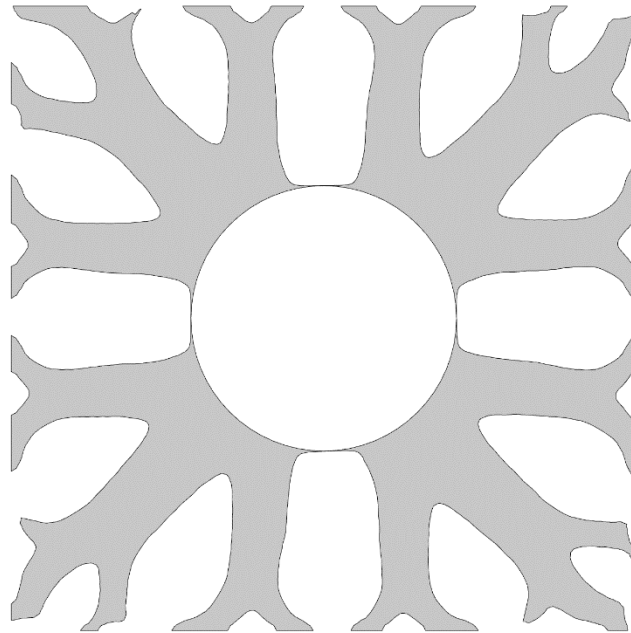


Figure 2.9. TO design for 20mm square and average material factor of 0,5.

### **2.2.2 Simulation results.**

Prior to the real-world testing the developed topology optimized heatsink design were also tested in a 3D simulation environment. The simulated testing was done using *Heat Transfer in Solids and Fluids (ht)* and *Laminar Flow (spf)* physics modules of COMSOL similarly to the attempts at 3D topology optimization. These modules allow to simulate heat transfer between different fluid and solids while also simulating the fluid flow surrounding the objects.

To decrease the computational time of the testing simulations built-in physics-controlled mesh size *Normal* was used. Built-in mesh sizes in COMSOL do not have exact mesh sizes associated with them but generate the size based on physics problem(s) being solved and internal logic implemented in the software. Also air domain with smaller diameter than the propeller, 40 mm compared to 76 mm, was used. The use of laminar flow was also a simplification as in most real world uses cases airflow created by the drone's motor are affected by many external factors and can be turbulent.

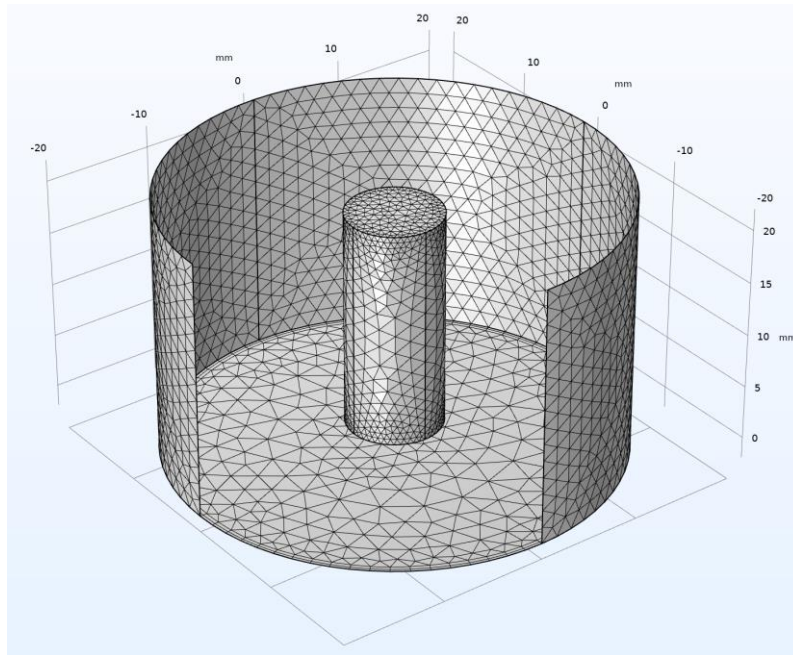


Figure 2.10. Mesh for the motor temperature simulation.

Initially a simulation was created without a heatsink to get a baseline for the motor's thermal performance. The mesh generated for the baseline test can be seen on the Figure 2.10 where the top and one side have been hidden to make the motor visible. The simulation was created in a way where it would be easy to add the optimized heatsinks designs for evaluation later. All the parameters and environmental conditions configured for this baseline simulation would remain the same for all simulations with the TO heatsink designs.

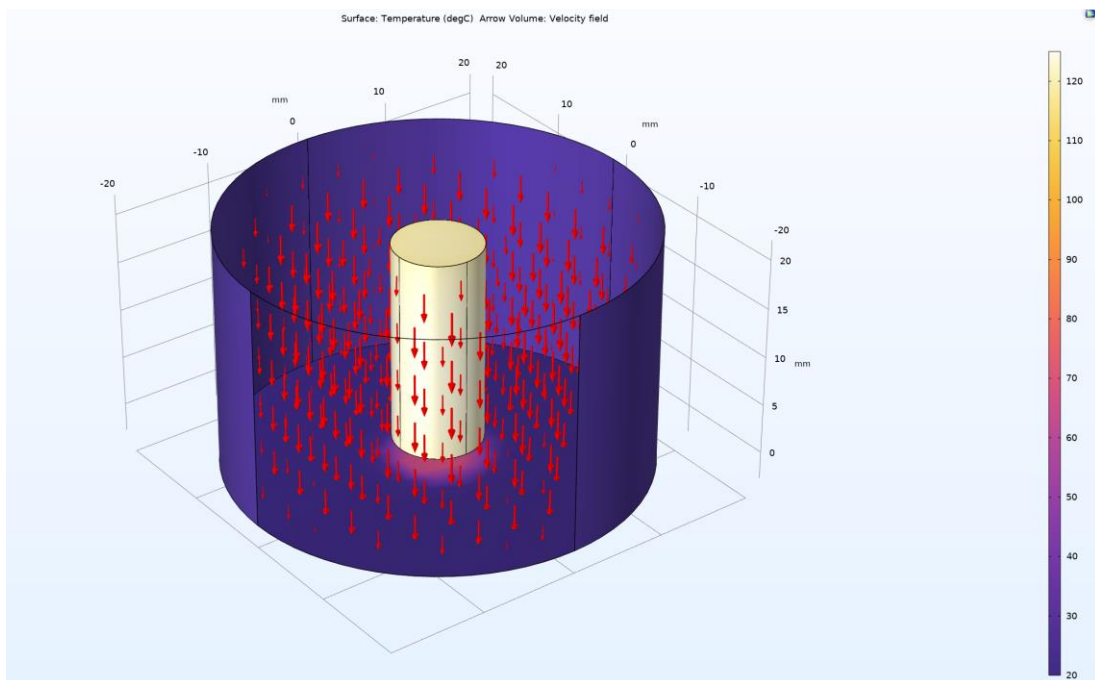


Figure 2.11. Thermal performance of the drone motor without a heatsink.

For the simulations the motor was simplified to be an uniform steel cylinder with a constant thermal output of 10 W similarly to the optimization process. The speed of average airflow generated by the moving propeller was set to 9,14 m/s as was calculated previously under the Physics Configuration point. The simulation conditions were setup as close to the TO generation process as possible.

From Figure 2.11 it can be seen that without a heatsink surface temperature of the motor would be slightly over 120 °C. Maximum surface temperature at one point was 121,38 °C. Sliced view of the motor showed the internal temperature of the motor was also evenly around the 120 °C value. The lack of any points with peak temperatures values was due to how the motor was simplified for the simulation.

Even though the used datasheet [32] does not specify the allowed working temperature for the drone motor 120 °C can be considered to be too high. This result demonstrates well the shortcomings of these kind motors and why heatsinks are required. Even if the airflow speed would be faster at the same thermal losses the temperature would still be quite high. For example, simulation ran at air speed of 16 m/s gave a result where the motor maximum surface temperature was 87,42 °C. Heatsinks or other methods need to be used for motor cooling as increasing the airflow just for this purpose is not possible due to drones working principles.

As the next step heatsink designs were inserted into the baseline simulation to evaluate the designs performance. Most heatsink designs had thin areas near the motor that could easily break. To make sure the heatsinks would not break during real-world handling extra cylindrical "sleeves" as parts of the heatsinks were added around the motor to increase the mechanical strength. These "sleeves" were added in the simulation testing to make the result more comparable to the real testing that came later. Attempts were made to add these already in the TO process as regions of predefined densities. As these stopped the optimization for working it was decided that these would be added later manually.

On Figure 2.12. an example of drone motor thermal performance can be seen. This example shows that the heatsink with diameter of 15 mm and allowed volume factor of 0,5 reduced the motor temperature over 40 °C. COMSOL plotted the maximum surface temperature to be 73,77 °C. Maximum motor surface temperature for other topology optimized heatsink design variants are brought out in Tables 2.6 and 2.7.

As the airflow was simulated to be laminar there were no turbulency shown to be generated when it passed between the heatsink fins. Simulations showed the airflow between the fins to be about two times slower than the average inflow that was configured.

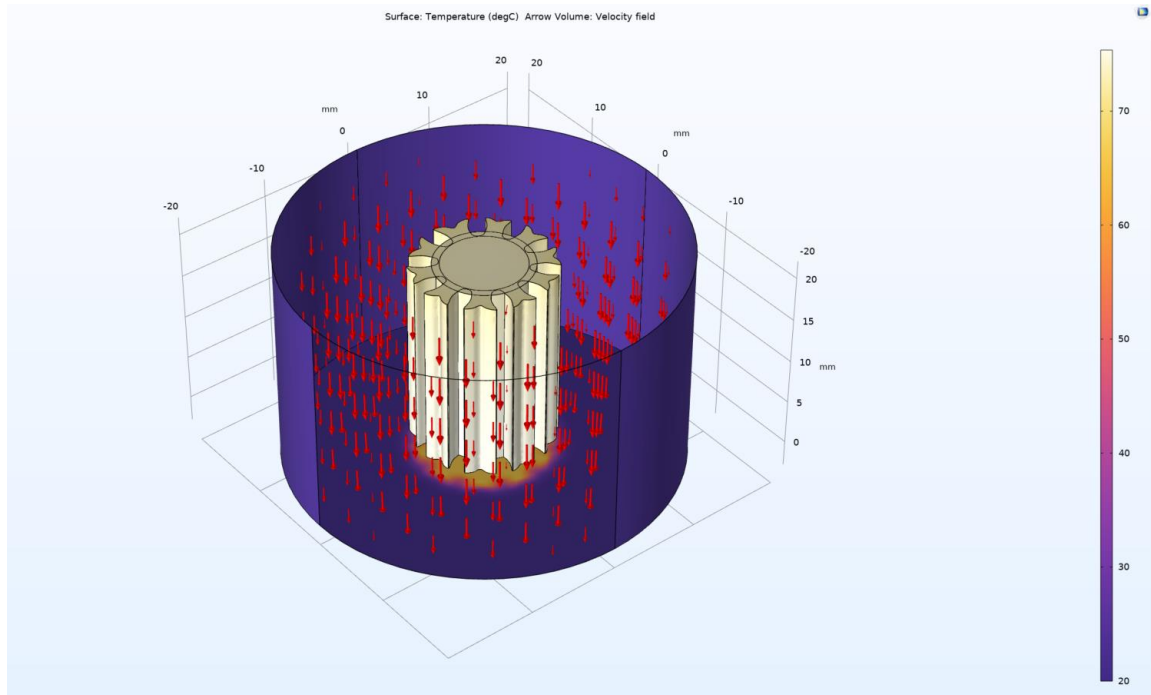


Figure 2.12. Simulation results for 15 mm diameter heatsink with maximum average volume factor of 0,5.

Table 2.6. Simulation results for when circular heatsink designs were used.

<b>Diameter [mm]</b>	<b>Maximum average volume factor</b>	<b>Maximum surface temperature [°C]</b>	<b>Theoretical mass [g]</b>
12	0,5	120,52	2,54
15	0,35	80,46	2,69
15	0,5	73,77	3,89
15	0,65	69,89	5,52
20	0,35	48,53	4,94
20	0,5	43,06	7,50
20	0,65	46,55	10,21
25	0,35	38,05	7,98
25	0,5	33,64	12,11
25	0,65	34,07	16,14

Table 2.7. Simulation results for when square heatsink designs were used.

<b>Square side length [mm]</b>	<b>Maximum average volume factor</b>	<b>Maximum surface temperature [°C]</b>	<b>Theoretical mass [g]</b>
12	0,5	96,38	2,97
15	0,5	56,96	5,13
20	0,5	36,80	10,20
25	0,5	27,59	15,70

From table 2.6 and 2.7 it can be seen that both the heatsink diameter and average volume factor have a significant effect on the topology optimized heatsink designs. The 12 mm heatsink did not improve the motor thermals significantly, temperature stayed at over 120 °C. Increasing the diameter to 15 mm already gave noticeable improvement. Enlarging the diameter by 3 mm reduced motor temperature about 50 °C, depending on the allowed volume factor. Theoretical masses for the heatsinks were taken from the simulation software with the material for the designs assigned to be aluminium.

Increasing the diameter to 20 mm reduced the temperature further down to under 50 °C. For this size heatsink unlike with the smaller heatsinks increasing the volume factor from 0,5 to 0,65 did not improve the thermal performance instead impaired it, 46,55 °C instead of 43,06 °C. Heatsink diameter increase to 25 mm improved the temperatures to be below 40 °C.

Square variants showed to be able to offer better cooling capabilities than their circular counterparts. Compared to the same volume factor circular heatsinks the temperature reductions were about 6 to 24 °C. This improvement is due to square variant having bigger design space meaning more mass and surface area could be added by TO with the same volume factor.

As drones are sensitive to weight, especially small drones like DJ Tello, adding weight above over 6 g per heatsink is unreasonable in this case. Adding more weight would lead to whole drone weight increasing over 30 % just for improving thermal performance. Depending on the drone size and application saving weight can be more important than achieving the best possible thermal performance. For calculating and analysing the mass to temperature improvement ratio the following formula was used:

$$R = \frac{m_{heatsink}}{\Delta t} = \frac{m_{heatsink}}{t_{base\_motor} - t_{motor}} \quad (2.12)$$

Where

$m_{heatsink}$  – mass of the heatsink, g,

$\Delta t$ - temperature difference, °C

$t_{base\_motor}$  – baseline of motor temperature without heatsinks, 121,38 °C,

$t_{motor}$  – motor temperature with the tested heatsink, °C.

Table 2.8. Mass needed for 1 °C of temperature improvement, circular TO heatsinks.

Diameter [mm]	Maximum average volume factor	R [mg/°C]
12	0,5	-
15	0,35	65,7
15	0,5	81,7
15	0,65	107,2
20	0,35	67,8

Table 2.9. Mass needed for 1 °C of temperature improvement, square TO heatsinks.

Square side length [mm]	Maximum average volume factor	R [mg/°C]
12	0,5	118,8
15	0,5	79,6

The  $R$  values in Tables 2.8 and 2.9 were calculated based on the information from the previous two tables. Maximum surface temperature of 121,38 °C from simulation without heatsink was used as the baseline temperature  $t_{base\_motor}$  for these calculations. The ratios were not calculated for heatsinks with masses over 6 g and for 12 mm diameter heatsinks it was left uncalculated as there was no significant thermal improvement according to the simulation.

From the mass-temperature ratio calculation result it can be seen that 15 and 20 mm diameter heatsinks with volume factor of 0,35 are the most optimal. Their performance ratios are under 70 mg/°C. They theoretically improve the motor temperature the most for the least amount of mass needed to be added to the drone. Added mass of square designs are somewhat justifiable as these designs' variants have equal or better mass to performance ratio to the radial design counterparts.

### 2.2.3 Parameter optimization for comparison

To get better insight to if and what potential benefits topology optimization offers simple 12 fin parameter optimized (PO) heatsinks designs were also quickly created for comparison. Fin amount was set to 12 as is a similar amount to the number of main branches of smaller TO designs and it also made the PO simpler to execute. These designs were also generated in 2D and tested in the simulated 3D space after their creation.

PO heatsinks design were created using the *Optimization* tool in COMSOL. This tool allows the optimization of different user defined parameters based on an objective function like for TO. In this case the objective function was set to be minimization of the average temperature of the motor that was again simplified to be a steel cylinder. The fin width and fin outer length from the motor centre were set as the parameters to be optimized.

So that the PO heatsinks would be similar size and weight to the TO ones the outer diameter was either limited maximum of 12 or 15 mm. In both cases the optimization process gave final values that were equal to maximum allowed diameter. Fin width on the other hand did change and gave result shown in table 2.10. On Figure 2.13. PO heatsink with allowed outer diameter of 15 mm can be seen.

Table 2.10. Simulation results for when PO heatsink designs were used.

<b>Diameter [mm]</b>	<b>Fin width [mm]</b>	<b>Maximum surface temperature [°C]</b>	<b>Theoretical mass [g]</b>	<b>R [mg/°C]</b>
12	2,425	82,51	3,13	80,5
15	2,6	65,21	5,79	103,1

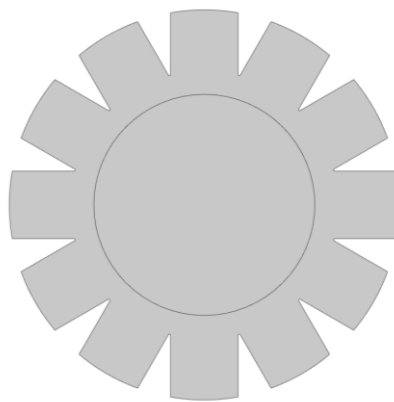


Figure 2.13. Parameter optimized heatsinks with allowed outer diameter of 15 mm.

Based on the temperature and mass to performance ratio given in Table 2.10 PO design are quite comparable to some of the designs gotten with topology optimization in terms of this ratio. The 12 mm diameter PO heatsinks shows to have better performance than both the radial and square TO heatsinks with the same size limit. Its thermal performance is not far off from the 15 mm TO heatsinks with volume factor of 0,35 but achieves it at a larger weight.

Regarding the computational time, PO heatsink design generation took less time than with TO. 1 to 2 minutes compared to 30 to 60 minutes required to complete TO calculations for optimal material distribution. While PO is a lot simpler and faster to run and setup than TO it could also be seen that simplicity is also its downside for the user. While the process itself easy to setup the main hurdle comes when parameterizing the geometry of the heatsink. It needs to be done in away where search for different optimal parameters does not interfere with each other nor create and solid block or cylinder of material without fins. Also, further so called fin branching is difficult to ingrate into the parameterization of the geometry elements. More work falls on the user to figure how to make the tools generate optimal geometry.

## 3. TESTING

### 3.1 Manufacturing of the heatsink designs.

As mentioned before the optimized heatsinks for multicopter motors were manufactured using metal additive manufacturing. SLM Solution 280 2.0 SLM printer available at Taltech [39] was used for this. This printer is able to print variety of alloys of stainless steel, aluminium, silver and titanium.

All together 9 of the created heatsink designs were manufactured for testing. Before they were manufactured modification were done to make them the fit the testing frame and have slot for temperature sensor. Slot was created from the base of the heatsink where a PT1000 temperature sensor could slide into and fit between the motor and heatsink. The slot for the sensors is pictured on Figure 3.1. The same figure also shows how the centre cylinders were made 5 mm longer to be able to attach the heatsinks to the frame.

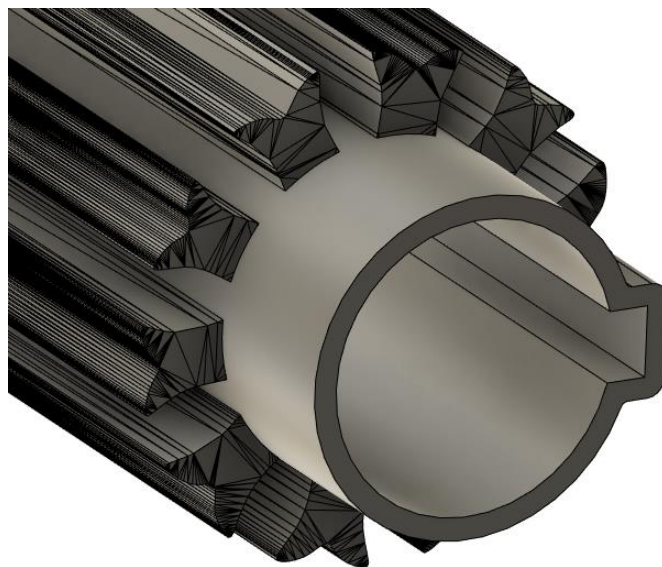


Figure 3.1. Depiction of modification made to all the heatsinks for testing.

On Figure 3.2. the heatsinks can be seen attached to the circular build platform after they had been printed together with some other parts. They were sawn off the platform and excess support material was removed with pliers.

After manufacturing the heatsink their inner walls were sanded down by hand to make the motors fit inside. Like with other additive manufacturing methods SLM printed parts also shrunk down when the material cools down meaning wholes and other cavities get smaller.



Figure 3.2. SLM printed heatsink designs attached to the build platform.



Figure 3.3. Separated heatsinks.

## 3.2 Testing setup and methodology

For testing a frame needed to be created that could hold the drone motor and heatsink in place while tests were ran. This frame would be attached to aluminium profiles that offer enough weight to hold the setup from lifting up from the thrust created by the propeller attached to the running drone motor. This frame, pictured on Figure 3.4, was created by the author using Autodesk Fusion 360.



Figure 3.4. Testing frame.

The created custom frame lifts the bottom of the motor about 60 mm up from the frames mounting surface. Frame was split into 3 parts, 1 centre part and 2 legs, to make its manufacturing easier and more material efficient when using plastic 3D printer. Centre part of this frame supports the motor in the right place inside the heatsinks and has necessary holes for passing through the motor and temperature sensor cables. Manufactured and assembled frame can be seen on Figure 3.5. TE Connectivity NB-PTCO-157 [40] resistive platinum sensors were used during the testing. This sensor has a nominal resistance of 1 k $\Omega$  and is suitable for measuring range of -50 to 600 °C. These sensors have measurement accuracy according to the formula  $\pm (0,3 + 0,005 \cdot T)$  °C. Where  $T$  is the temperature measurement captured.

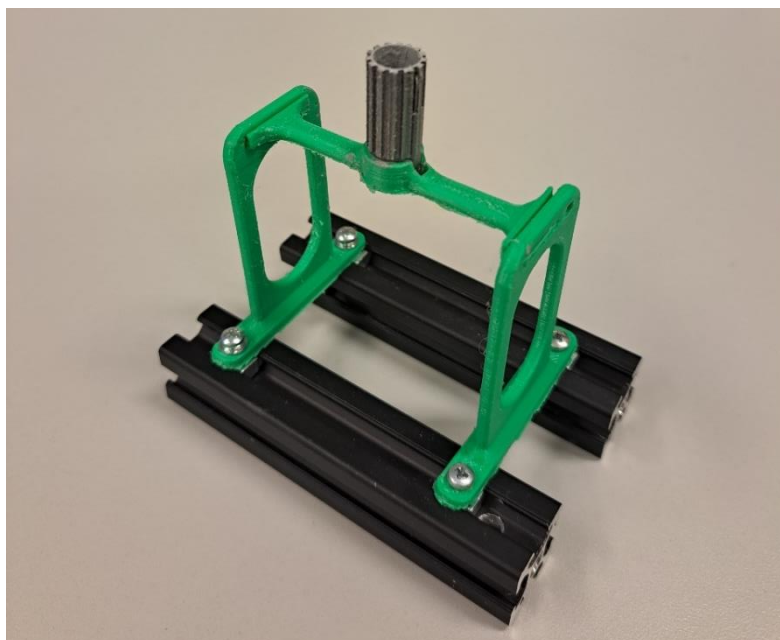


Figure 3.5. Printed out frame design with one heatsink attached.

As the next step wires were soldered to the temperature sensor. Two wires were soldered to each leg of the sensors to make it possible to use 3-wire resistance measuring. 3-wire measuring helps to compensate for the voltage drop on the wires giving a more accurate temperature read. Additionally, this increased number of sensor wires also meant that the centre of the frame needed to be slightly modified by hand to make sure the wires fit more easily through the centres base.

On figure 3.6 the fully assembled testing frame setup can be seen. To be sure the heatsinks and motor had good thermal contact thermal paste was apply between. Thermal paste was applied to the inside of the heatsink so that when the motor was inserted from the bottom it pressed out the excess amount of thermal paste. This helped to make sure that all of the heatsinks had similar thermal contact with the motor during tests.

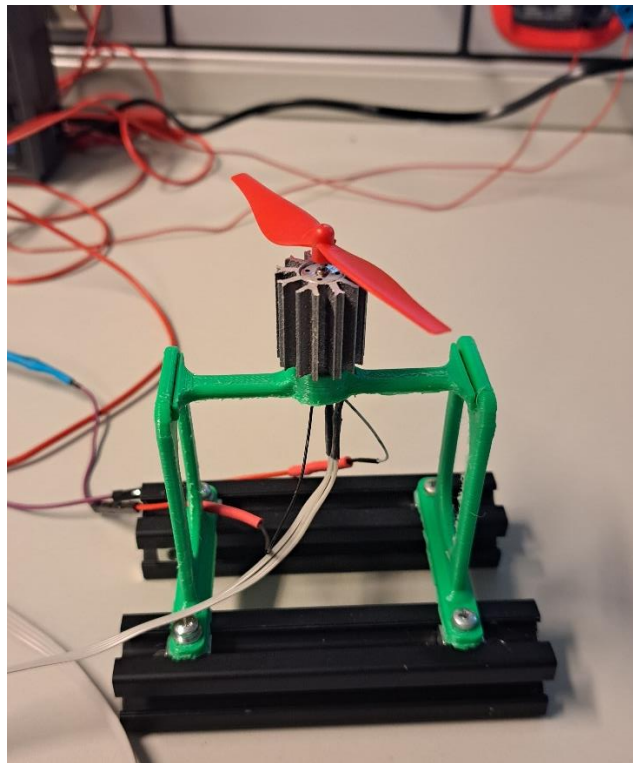


Figure 3.6. Frame assembled with motor, heatsink, sensor and propeller.

The motor was supplied with a controllable laboratory power supply that could run either in constant current or voltage mode. Additional multimeter was used to measure the actual voltage applied to the motor windings. This was done as the power supply reported slightly higher output voltage than what reached the motor. Data logger was used to gather the temperature data from both the motor surface and of ambient temperature inside the room. The assembled whole testing setup can be seen on Figure 3.7. below.

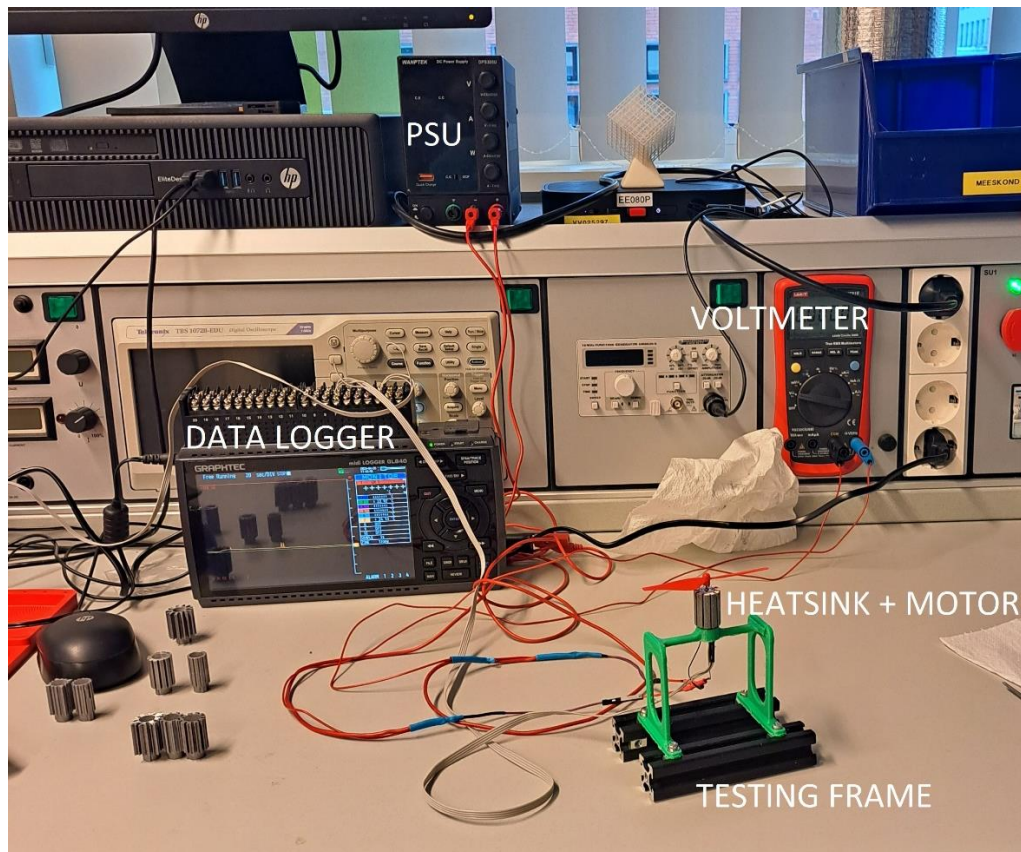


Figure 3.7. The whole testing setup.

For evaluating the performance of each of the created and manufactured heatsinks designs test were run to see how each of the designs can handle the same thermal load from the motor. To achieve this the motor was ran at the same constant input voltage of 3,69 V from the power supply. This voltage was chosen as 3,7 V is nominal rated voltage [35] for this model of drone motor. Slightly higher voltage of 4 V was also tried but it ended up damaging and destroying the motor.

After configuring the power supply to the specified voltage the testing started. For each of the heatsinks a thermal loading test was run and the motors drawn current and surface temperature captured. Attention was also directed to gauging a general overview of the time needed to reach steady state temperatures with each of the heatsink.

Due to the small scale and construction there was no reasonable or reliable way of measuring the temperature of internal components and the surface temperature readings had to be considered to be enough. Only one measuring spot was used as the construction of the motor is uniform and symmetrical meaning that there should not be any major hot spots on these motors. The author estimates that measuring the motor

surface temperature gives temperature results about 10 to 20 °C lower than the actual internal temperature of the motors. This due to the thermal resistance of the motor outer shell and the air caps between the different components. The thermal resistance of the motor stator should not affect the temperature rating much as seen on Figure 1.4. it is in the middle of the motor. Meaning this type of DC motor can be considered to be an enclosed outer rotor motor.

### 3.3 Testing results

Test were ran at least 5 minutes or until steady state temperature was reached with each of the heatsinks designs. This relatively short test time was possible due to the low mass of the motors that meant they heated up in a short period of time. After each test the motor was let to cool down to ambient before the next heatsink was installed and tested. The ambient temperature was about 24 °C while the tests were conducted. To have a reference a test was also ran to see the motors surface temperature without an heatsinks installed. The results from this test can be seen in Table 3.1. Without a heatsink motor surface temperatures reached 62,6 °C from that it can be derived that the motors internal temperatures would be over 80 °C.

During the first test it was also noticed that after switching of the power to the motor the motor surface temperature increased as there was no airflow anymore. The temperature rose for some time before starting to come down. The peaks of this temperature were recorded as it can give and insight to how much thermal energy was stored inside the motor internals. Larger increase in temperature after airflow stopped meaning more trapped heat.

Table 3.1. Testing results without a heatsinks installed.

	<b>Current [A]</b>	<b>Motor surface temperature [°C]</b>	<b>Motor temperature peak after test [°C]</b>
Without heatsink	2,03	62,6	70,9

Table 3.2. Testing results for circular TO heatsinks designs.

<b>Number on graph</b>	<b>Diameter [mm]</b>	<b>Maximum average volume factor</b>	<b>Current [A]</b>	<b>Motor surface temperature [°C]</b>	<b>Motor temperature peak after test [°C]</b>
1	12	0,5	2,03	45,4	51,0
2	15	0,35	2,17	42,7	47,2
3	15	0,5	2,17	40,5	43,1
4	15	0,65	2,16	36,2	37,8
5	20	0,35	2,19	32,5	34,3

Table 3.3. Testing results for square TO heatsinks designs.

Number on graphs	Side length [mm]	Maximum average volume factor	Current [A]	Motor surface temperature [°C]	Motor temperature peak after test [°C]
6	12	0,5	2,08	43,9	49,4
7	15	0,5	2,19	34,5	36,2

Table 3.4. Testing results for PO optimized heatsink designs.

Number on graphs	Diameter [mm]	Current [A]	Motor surface temperature [°C]	Motor temperature peak after test [°C]
8	12	2,04	49,7	54,1
9	15	2,06	42,9	45,3

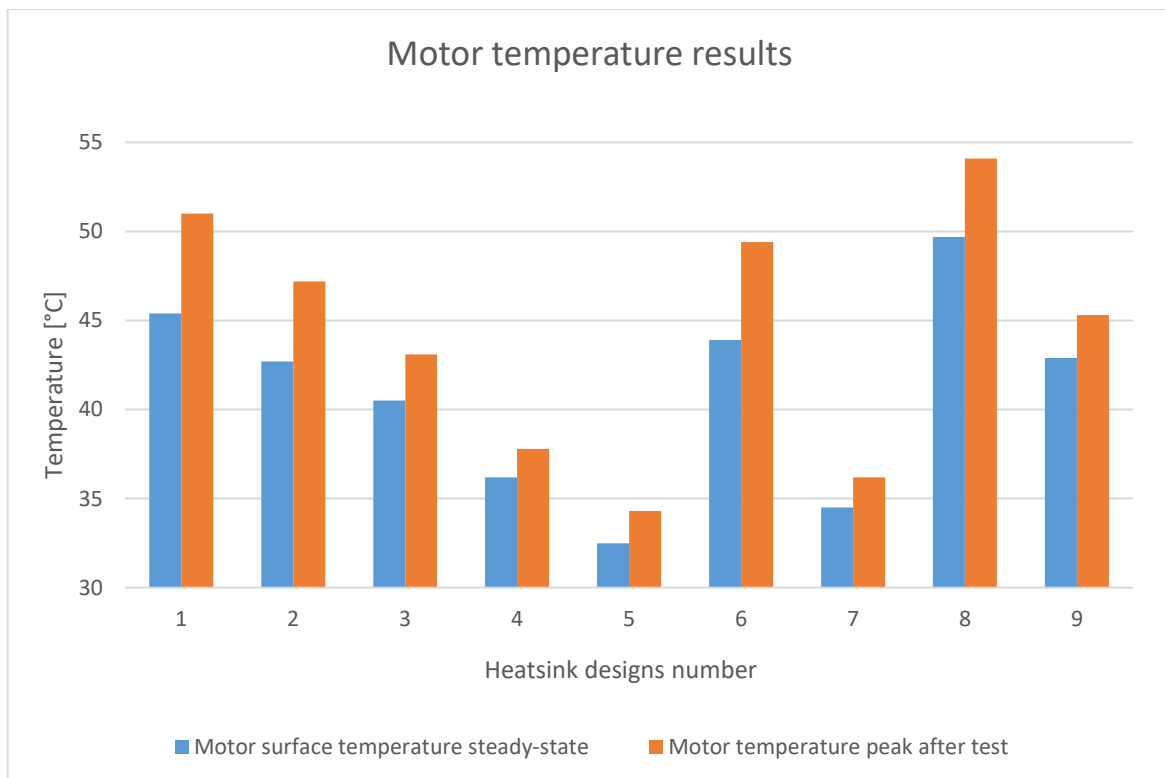


Figure 3.8. Visualization of testing results.

From tables 3.2, 3.3 and 3.4 results for heatsinks test can be seen. These results are visualized on Figure 3.8 that both shows motors steady state temperatures and peaks after the motor was stopped. Compared to the simulated testing results the temperature are lower and the differences between different designs smaller. This is since the motor was supplied with only 8 W of power meaning the thermal losses are smaller than were configured in the simulation tests. Another reason for this difference is how the simulations simplified the motor as exact properties of the motor are difficult to model. From these table it can also be seen that unlike with simulation all the heatsinks were able to noticeable reduce the motor surface temperature.

As seen with simulations the real world results follow a similar pattern where the designs with bigger gauge measurements and allowed volume factors were able to achieve lower temperatures. Additionally, for the so called bigger heatsinks the temperature increase after airflow was stopped were the smaller, around 2 °C compared to the 8,29 °C of the base test. Comparing motor current also shows that all the topology optimized heatsinks, except the ones with gauge measurements of 12 mm, allowed the motors to run at higher current meaning more potential power and performance from the motor. This current increase was up to 8 %. This shows that while 12 mm designs are usable these are not the most optimal if some extra performance/efficiency is needed. The square TO heatsinks shows larger temperature improvements over their circular counterparts especially for the design with 15 mm side length.

While parameter optimized heatsinks show improved temperature compared to the base test both the current and temperature measurements show that they are inferior to the TO designs. Currents were close to base result of 2,03 A and temperatures to the worst performing TO heatsinks. They achieved these results with higher masses than their TO counterparts.

Additionally, while not measured it could be seen that with the so called bigger heatsinks the steady state temperatures were reached much slower. With the smaller heatsinks the temperature increase was significantly more rapid.

Table 3.5. Mass needed for 1 °C of temperature improvement, circular TO heatsinks.

Number on graph	Diameter [mm]	Maximum average volume factor	Mass [g]	Temperature improvement [°C]	R [mg/°C]
1	12	0,5	1,7	17,2	98,8
2	15	0,35	2,1	19,9	105,5
3	15	0,5	2,5	22,1	113,1
4	15	0,65	4,6	26,4	174,2
5	20	0,35	4,0	30,1	132,9

Table 3.6. Mass needed for 1 °C of temperature improvement, square TO heatsinks.

Number on graph	Side length [mm]	Maximum average volume factor	Mass [g]	Temperature improvement [°C]	R [mg/°C]
6	12	0,5	2,7	18,7	144,4
7	15	0,5	4,1	28,1	145,9

Table 3.7. Mass needed for 1 °C of temperature improvement, PO heatsinks.

Number on graph	Diameter [mm]	Mass [g]	Temperature improvement [°C]	R [mg/°C]
8	12	2,5	12,9	193,8
9	15	4,6	19,7	233,5

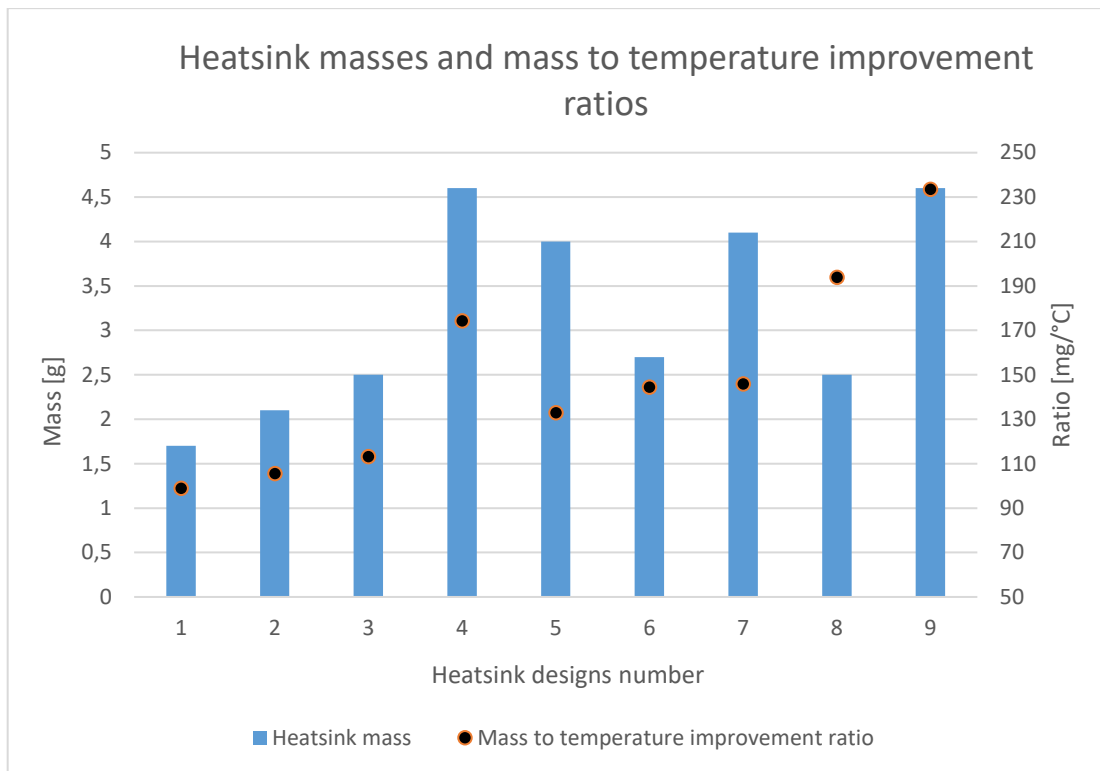


Figure 3.9. Graph of heatsink masses and their mass to temperature ratios.

Calculating mass to temperature improvement ratios, calculation result in Tables 3.5, 3.6 and 3.7, for the real-world testing with formula 2.12 shows different results compared to the simulation. Heatsinks masses and ratios are visualized on Figure 3.9. Generally, the real heatsinks needed more mass to gain a unit of performance. One of the biggest differences was that the 12 mm diameter topology optimized heatsink in real testing improved the motor thermals while in simulation it did not affect them at all. It also gave the most optimal thermal performance for its mass out of the tested heatsink designs. But as mentioned before the 12 mm designs does not seem to offer any performance or efficiency benefit over the base test. This means that the heatsinks with diameter of 15 mm and volume factor of 0,35 can be considered the most optimal as test with it also showed motor current increase of about 7 % at a lower temperature. The drone would be only about 1,8 % heavier with four of the mentioned 15 mm heatsinks installed compared to when it were to be equipped with the 12 mm ones.

At a first glance from the circular TO heatsinks mass to performance ratios it would seem that these ratios increase in a relatively linear pattern with the increasing mass of the heatsinks, but the other results show otherwise. For both of the square TO heatsinks the mass to performance ratios are almost the same. The square heatsinks compared worse to the circular TO heatsinks with similar masses. The results from the PO heatsink tests highlight the weight advantages of TO optimization as the PO designs required the largest among of mass to reduce motor temperature by 1 °C.

In conclusion, the testing result show that created topology optimized heatsink designs show are effective and capable of noticeable reducing temperatures of these small drone motors. The heatsinks are able do this while also slightly improving the potential performance and efficiency of the motor. Topology optimization is able to produce designs more effective both in terms of term performance and weight compared to the more classical parameter optimization. Testing showed that the smallest size heatsink was the lightest and seemed to offer the most amount of thermal improvement for its mass. While it was most optimal in terms of mass the motor surface temperatures were the highest and the current lowest. This meant that the slightly bigger heatsink with diameter of 15 mm and volume factor of 0,35 could be considered the most optimal. It can theoretically improve the motor performance and thermals the most for least amount of mass added.

### **3.4 Suggestions for further development**

As there were multiple simplification and assumptions made during the topology optimization process and simulations then improvement could be made in future research. One of the major improvements that could be made would be more precise modelling of the motor and its properties. This would allow the simulations to give a more accurate overview of the motor and its thermal performance with the heatsinks being designed. Also, the motor thermal output should be modelled based on analysing actual information gathered from drone flight data not maximum power situation like was done in this case.

In terms of the topology optimization process while moving it over to 3D simulation space is difficult for this kind of an active cooling solution it could be automated further. Under automation it is meant that if possible, a hybrid of topology and parameter optimization might be able to be created. This would allow the software itself change and test some parameters like the designs space size and volume factor that currently were manually changed by the user. This could help save on human labour and produce the most optimal solutions for problems being solved.

Finally, these heatsink design should be tested in real world application where a drone is used for some purpose. This would give an additional change of analysing if and how big benefits the use heatsinks can give. For example, do the temperature improvement shown in the laboratory setting carry over to real performance and electrical efficiency increases.

## SUMMARY

The aim of this thesis was to design topology optimized heatsinks for small drone motors with the end goal of improving the motor performance. COMSOL Multiphysics Simulation Software was used to generate the designs discussed and analysed in the thesis. This work was conducted out of authors personal interest and universities desires to research ways of improving motor thermals with moder technological solutions.

As the first step for completing the set thesis aims the background of drone and heatsinks design was researched. Focus was on the working principle of topology optimization and how it can be applied to thermal designs. It was concluded that while TO has mostly been used for mechanical design newer research has proven its applicability in heatsinks design. The usability of this kind of optimization is also supported by the increased accessibility to different additive manufacturing technologies. Literature review helped to guide and better understand how the TO process should be setup.

Variety of heatsinks designs were generated using the TO module of COMSOL software for the small DJI Tello sized drones' motors that are used in Taltech projects. The aim of TO process was to find the most optimal material distribution inside the given design space for achieving the most thermally conductive heatsink. The different heatsink designs were generated by changing the designs space size or the constraints set for the optimization process. Two parametrically optimized designs were also created for being able to see if and what benefits using TO offers over more classical optimization methods. After creating the designs, they were tested in a simulated software environment to see what theoretical performance should be expected from later testing them in real-world. The theoretical mass of the heatsinks was calculated using CAD software and their thermal performance improvement per mass added calculated. This was done to eliminate heatsinks with unreasonable larges masses for the given drone platform. Those heatsinks were not manufactured. This performance ratio also gave a better insight into what TO designs should be the most optimal compared to the others created.

Out of the created designs 9 heatsinks were manufactured and tested. 7 of these designs were gotten using TO and 2 of them were the PO designs created for comparison. All of the tests were done by running the motor at a constant voltage for it to generate the same amount of heat for each test. As measuring the motors inner temperature was not possible or reasonable the outer housings surface temperature was recorded. Also, the current drawn by the motor was measured as it gives an indication to potential

performance benefits of the heatsinks. Testing results and mass to performance improvement ratio calculations showed that TO has a noticeable weight benefit over PO. Same thermal performance was reached with lighter heatsinks. The tests also showed that in terms of mass the square TO designs are less optimal than the circular ones for this application. Test showed that the most optimal design was a circular topology optimized heatsink with diameter of 15 mm that was allowed to fill out 35 % of the design space with material.

In conclusion the aims of the thesis were achieved. Variety of heatsink designs for drone motors were created using topology optimization. The generated designs were tested both in simulated and real environments. Results were analysed and a most optimal design was selected. It was concluded that the optimization process can be improved further by more accurately modelling the drone motor and the thermal load generated by it. Also, the heatsinks designs should be tested in real-world applications to see if the seen potential benefits carry over to real use as well.

# KOKKUVÕTE

Antud lõputöö eesmärgiks oli projekteerida väikestele drooni mootoritele topoloogia optimeeritud jahutid sihiga parandada mootorite jõudlust. COMSOL Multiphysics Simulation tarkvara kasutati, et jahutite disainide loomiseks ja nende analüüsimiseks. Töö viidi läbi autori isiklikust huvist 3D printimise ja selle rakendamise vastu ning ülikooli soovist uurida elektrimootorite potentsiaalseid jahutuslahendusi, mis kasutavad ära moodsaid tehnoloogilisi lahendusi.

Eesmärkide täitmise esimeseks sammuks oli uurida droonide ja jahutite disainimise tausta. Keskenduti topoloogia optimeerimise tööpõhimõtetele ning kuidas seda oleks võimalik soojuslikes rakendustes kasutada. Jõuti järeldusele, et kuigi TO-d on olnud enamasti kasutusel mehaaniliste detailide projekteerimisel, näitavad uuemad uuringud, et seda on võimalik edukalt kasutada ka jahutite disainimisel. Seda liiki optimeerimise kasutatavust toetab ka suurenenud ligipääsetavus erinevatele materjali lisandliku tootmise tehnoloogiatele. Kirjanduse ülevaade aitas suunata ja paremini mõista TO-protsessi olemust ning seadistamist.

Mitmeid erinevaid jahutiti variante loodi DJI Tello suuruste droonide jaoks, mida Taltech oma projektides kasutab. TO protsessi eesmärgiks oli leida lubatud disainiruumi sees optimaalne materjalijaotus, mis annaks jahutile võimalikult suure soojusjuhtivuse. Erinevad disainid saadi disaini ala suuruse või optimeerimisprotsessi piirangute muutmise kaudu. Samuti loodi võrdluseks kaks parameetriselt optimeeritud jahutit, et näha, kas ja milliseid eeliseid pakub TO kasutamine võrreldes klassikaliseimate optimeerimise meetoditega. Loodud jahuti disaine testiti simuleeritud keskkonnas tarkvara sees, et näha millist tulemust võib neilt oodata hilisemas testimises laboris. Arvutati CAD-tarkvara abil välja jahutite mass ja võrreldi palju massi tuleb lisada iga disaini puhul, et tuua mootori temperatuur alla ühe kraadi võrra. See oli vajalik ka selleks, et elimineerida ebamõistlikult suurte massidega disainid, mis jäeti ka hiljem välja printimata. Massi ja temperatuuri suhe andis ka parema ülevaate ka missugused TO jahuti disainid on realselt kõige optimaalsemad.

Loodud jahutusradiaatori disainidest 9 valmistati ja testiti. Nendest 7 saadi topoloogia optimeerimise abil ja 2 parameetriselt optimeerimisega. Selleks, et kõikide katsete ajal tekitaks mootor sama palju sooja rakendati sellele sama konstantset pinget kõikide testide jooksul. Kuna mootori sisetemperatuuri mõõtmine ei olnud võimalik ega mõistlik mõõdeti mootori korpuse pinnatemperatuur. Samuti jäädvustati mootorit läbiv vool, sest see annab aimu radiaatorite potentsiaalsest mõjust mootori jõudlusele.

Katsetulemused ning massi ja temperatuuri paranemise suhted näitasid, et TO-I on võrreldes PO-ga märgatav kaalu eelis. Sarnased temperatuurid saavutati kergemate radiaatoritega. Testid näitasid ka, et ruudukujulised TO disainid on selles rakenduses vähem optimaalsed kui ringikujulised. Testid näitasid, et kõige optimaalsemaks saab pidada topoloogiaga optimeeritud radiaatorit 15 mm läbimõõduga, millel oli optimeerimisel lubatud täita materjaliga 35 % disaini alast.

Kokkuvõtteks saab öelda, et antud lõputöö eesmärgid saavutati. Topoloogia optimeerimise abil loodi droonimootorite jaoks erinevaid radiaatorite disaine. Loodud disaine testiti nii simuleeritud kui ka realses keskkonnas. Testide tulemusi analüüsiti ja valiti välja kõige optimaalsem disain. Jõuti järeldusele, et optimeerimisprotsessi saaks tulevikus täiendada mootorite ja nende töö täpsema modelleerimisega. Samuti tuleks radiaatoreid testida reaalsete droonidega, et näha kas ja kui suuri eeliseid need annavad realses kasutuses.

## LIST OF REFERENCES

- [1] "IEEE Standard for Drone Applications Framework," in IEEE Std 1936.1-2021.
- [2] Zifan Fang, Lei Yang, Daojia Du, Kongde He, Dalin Zhu and Yi Zhang, "Study on multi-objective topology optimization design for support structure," 2010 International Conference on Mechanic Automation and Control Engineering, 2010
- [3] F. Lange, C. Hein, G. Li, C. Emmelmann, "Numerical optimization of active heat sinks considering restrictions of selective laser melting", 2018 Fraunhofer Research Institution for Additive Manufacturing Technologies IAPT, Hamburg, Germany
- [4] M. S. Santhanakrishnan, T. Tilford and C. Bailey, "Multi-Material Heatsink Design Using Level-Set Topology Optimization," in IEEE Transactions on Components, Packaging and Manufacturing Technology, vol. 9, no. 8, pp. 1504-1513, Aug. 2019
- [5] A. Hafifi Zulkipli, T. Raj, F. H. Hashim and A. Baseri Huddin, "Characterization of DC brushless motor for an efficient multicopter design," 2016 International Conference on Advances in Electrical, Electronic and Systems Engineering (ICAEEES), Putrajaya, Malaysia, 2016, pp. 586-591.
- [6] K. L. Pham, J. Leuchter, R. Bystřický, V. T. Pham and N. N. Pham, "Design and Simulation System for Quadrotor UAVs," 2021 International Conference on Military Technologies (ICMT), Brno, Czech Republic, 2021, pp 1-5
- [7] J. -J. Xiong, N. -H. Guo, Y. -X. Hong and E. -H. Zheng, "Improved Position and Attitude Tracking Control for a Quadrotor UAV," 2019 Chinese Automation Congress (CAC), Hangzhou, China, 2019, pp. 4197-4201.
- [8] G. SHAN, Y. Zhang, Y. Gao, T. Wang and J. Chen, "Control of Quadrotor Drone with Partial State Observation via Reinforcement Learning," 2019 Chinese Automation Congress (CAC), Hangzhou, China, 2019, pp. 1965-1968
- [9] D. Valencia and D. Kim, "Quadrotor Obstacle Detection and Avoidance System Using a Monocular Camera," 2018 3rd Asia-Pacific Conference on Intelligent Robot Systems (ACIRS), Singapore, 2018, pp. 78-81.
- [10] N. Yamamoto and N. Uchida, "Improvement of Image Processing for a Collaborative Security Flight Control System with Multiple Drones," 2018 32nd International Conference on Advanced Information Networking and Applications Workshops (WAINA), Krakow, Poland, 2018, pp. 199-202.
- [11] D. T. Larsson, C. H. Nguyen and P. Artemiadis, "Modeling and Control of Mid-flight Coupling of Quadrotors: A new concept for Quadrotor cooperation," 2020 International Conference on Unmanned Aircraft Systems (ICUAS), Athens, Greece, 2020, pp. 310-315.

- [12] Droon.ee, *Tello*, Available: <https://droon.ee/toode/tello/?lang=en>. Used 21.01.2023.
- [13] Ric Motor, *Coreless motor RIC-8520D*, Available: <https://www.ricmotor.com/details/8520-coreless-motor>. Used 21.01.2023.
- [14] D. Collins, Motion Control Tips, *What are coreless DC motors?*, Available: <https://www.motioncontroltips.com/what-are-coreless-dc-motors/>. Used 21.01.2023.
- [15] R. Bornoff, J. Parry, M. Sapiano and M. Warner, "A Geometry Remodelling Approach to Heatsink Optimisation," 2020 26th International Workshop on Thermal Investigations of ICs and Systems (THERMINIC), Berlin, Germany, 2020, pp. 1-6.
- [16] W. Luiten, "Multi Software Thermal Design Optimization," 2020 26th International Workshop on Thermal Investigations of ICs and Systems (THERMINIC), Berlin, Germany, 2020, pp. 1-6
- [17] S. Otake et al., "Heatsink design using spiral-fins considering additive manufacturing," 2019 International Conference on Electronics Packaging (ICEP), Niigata, Japan, 2019, pp. 46-51
- [18] M. P. Bendsøe and O. Sigmund, "Topology Optimization: Theory Methods and Applications," Berlin, Germany:Springer, 2004.
- [19] K. Svanberg, "The method of moving asymptotes—A new method for structural optimization", *Int. J. Numer. Methods Eng.*, vol. 24, no. 2, pp. 359-373, Feb. 1987.
- [20] M. Santhanakrishnan, T. Tilford and C. Bailey, "On the application of topology optimisation techniques to thermal management of microelectronics systems," 2016 17th International Conference on Thermal, Mechanical and Multi-Physics Simulation and Experiments in Microelectronics and Microsystems (EuroSimE), Montpellier, France, 2016, pp. 1-7
- [21] B. Xue, F. Dong, H. Zhong and Z. Liu, "Topology optimization design of trussed bracket of thruster on satellite," 2020 5th International Conference on Mechanical, Control and Computer Engineering (ICMCCE), Harbin, China, 2020
- [22] J. Hub, "A Study on Topology Optimization of Airplane Air Brake Bracing Beam," 2019 International Conference on Military Technologies (ICMT), Brno, Czech Republic, 2019, pp. 1-4 .
- [23] R. Bornoff and J. Parry, "An additive design heatsink geometry topology identification and optimisation algorithm," 2015 31st Thermal Measurement, Modeling & Management Symposium (SEMI-THERM), San Jose, CA, USA, 2015, pp. 303-308

- [24] H. P. de Bock, "Exploration of a Hybrid Analytical Thermal Topology Optimization Method for an Additively Manufactured Heat Sink," 2018 17th IEEE Intersociety Conference on Thermal and Thermomechanical Phenomena in Electronic Systems (ITherm), San Diego, CA, USA, 2018, pp. 761-767
- [25] H. Akhtar, H. Terry, P. Ioannou, L. Mills, S. Samanthula and A. Wise, "Additive Manufactured Heatsinks for Power Electronics Assemblies – Multi Physics Topology Optimisation," PCIM Europe digital days 2021; International Exhibition and Conference for Power Electronics, Intelligent Motion, Renewable Energy and Energy Management, Online, 2021, pp. 1-9.
- [26] A. Mueller, C. Buennagel, S. Monir, A. Sharp, Y. Vagapov and A. Anuchin, "Numerical Design and Optimisation of a Novel Heatsink using ANSYS Steady-State Thermal Analysis," 2020 27th International Workshop on Electric Drives: MPEI Department of Electric Drives 90th Anniversary (IWED), Moscow, Russia, 2020, pp. 1-5.
- [27] A. Syed-Khaja, D. Walawski, T. Stoll and J. Franke, "Is selective laser melting (SLM) an alternative for high-temperature mechatronic integrated devices? methodology, hurdles and prospects," 2016 12th International Congress Molded Interconnect Devices (MID), Wuerzburg, Germany, 2016, pp. 1-5.
- [28] L. Fuhui, K. Decheng, Z. Xiaoyu, M. Xiaowei and H. Ketai, "Mechanical properties and optimization of AlNiCo magnetic materials fabricated by selective laser melting," 2022 IEEE 17th Conference on Industrial Electronics and Applications (ICIEA), Chengdu, China, 2022, pp. 1283-1288.
- [29] S. Klengel, A. Krombholz, O. Schwedler and H. Busch, "Material characterization of copper structures for electronic systems manufactured by selective laser melting (SLM)," 2021 23rd European Microelectronics and Packaging Conference & Exhibition (EMPC), Gothenburg, Sweden, 2021, pp. 1-6.
- [30] COMSOL, *COMSOL Multiphysics® Simulation Software*, Available: <https://www.comsol.com/comsol-multiphysics>. Used 28.02.2023.
- [31] COMSOL Application Gallery, *Heat Sink*, Available: <https://www.comsol.com/model/heat-sink-8574>. Used 28.02.2023.
- [32] Humusoft, *COMSOL Multiphysics: Topology Optimization of Heat Sink, Part 1*, Available: <https://www.youtube.com/watch?v=ApXzfJROyLQ>. Used 12.12.2023.
- [33] Humusoft, *COMSOL Multiphysics: Topology Optimization of Heat Sink, Part 2*, Available: [https://www.youtube.com/watch?v=S\\_x\\_7cL8dl8&t=119s](https://www.youtube.com/watch?v=S_x_7cL8dl8&t=119s). Used 12.12.2023.

- [34] M. Sarap, A. Kallaste, P. S. Ghahfarokhi, H. Tiismus and T. Vaimann, "The Effect of Build Direction on the Thermal Conductivity of Additively Manufactured AlSi10Mg and Silicon-steel Samples," 2022 International Conference on Electrical Machines (ICEM), Valencia, Spain, 2022, pp. 538-543.
- [35] Global Sources, *Ineed Electronics 8520-155009-L570-145*, Available: <https://p.globalsources.com/IMAGES/PDT/SPEC/838/K1136645838.pdf>. Used 29.02.2023,
- [36] Ineed Electronics, *8mm Vibration Motor IND-YQ8520-001*, Available: <http://ee.ineed-motor.com/micro-motor/4-8mm-high-speed-versions/10mm-vibration-motor.html>. Used 29.02.2023.
- [37] Menzel Elektromotoren, *Energy efficiency classes for IEC motors*, Available: <https://www.menzel-motors.com/iec-motors/>. Used: 10.04.2023.
- [38] NASA Glenn Research Center, *Propeller Analysis*, Available: <https://www.grc.nasa.gov/www/k-12/airplane/propanl.html>. Used 30.03.2023.
- [39] Taltech, Department of Mechanical and Industrial engineering, Services, Available, <https://taltech.ee/en/department-mechanical-and-industrial-engineering/services>. Used 29.04.2023.
- [40] Farnell, *TE Connectivity NB-PTCO-157*, Available: <https://ee.farnell.com/sensor-solutions-te-connectivity/nb-ptco-157/rtd-sensor-thin-film-platinum/dp/2918450>. Used 03.04.2023.

## **APPENDICES**

3D models of the manufactured heatsinks and testing frame parts are included as appendices in separate files. The CAD models are in STL file format.

## **GRAPHICAL MATERIAL**